SOLUBLE AND PELLETABLE FACTORS IN PORCINE, CANINE AND HUMAN NOTOCHORDAL CELL-CONDITIONED MEDIUM: IMPLICATIONS FOR IVD REGENERATION

F.C. Bach[1,§], S.A.H. de Vries[2,§], F.M. Riemers[1], J. Boere[3,4,5], F.W.M. van Heel[1], M. van Doeselaar[2], S.S. Goerdayal[6], P.G.J. Nikkels[7], K. Benz[8], L.B. Creemers[5], A.F. Maarten Altelaar[6], B.P. Meij[1], K. Ito[2,5] and M.A. Tryfonidou[1,*]

[1]Department of Clinical Sciences of Companion Animals, Faculty of Veterinary Medicine, Utrecht University, Utrecht, the Netherlands
[2]Orthopaedic Biomechanics, Department of Biomedical Engineering, Eindhoven University of Technology, Eindhoven, the Netherlands
[3]Department of Biochemistry and Cell Biology, Faculty of Veterinary Medicine, Utrecht University, Utrecht, the Netherlands
[4]Department of Equine Sciences, Faculty of Veterinary Medicine, Utrecht University, Utrecht, the Netherlands
[5]Department of Orthopaedics, University Medical Centre Utrecht, Utrecht, the Netherlands
[6]Biomolecular Mass Spectrometry and Proteomics, Bijvoet Centre for Biomolecular Research, Utrecht Institute for Pharmaceutical Sciences and The Netherlands Proteomics Centre, Utrecht University, Utrecht, the Netherlands
[7]Department of Pathology, University Medical Centre Utrecht, Utrecht, the Netherlands
[8]TETEC AG, Reutlingen, Germany

[§] These authors contributed equally, shared first authorship.

Abstract

During intervertebral disc (IVD) maturation, notochordal cells (NCs) are replaced by chondrocyte-like cells (CLCs) in the nucleus pulposus, suggesting that NCs play a role in maintaining tissue health. Affirmatively, NC-conditioned medium (NCCM) exerts regenerative effects on CLC proliferation and extracellular matrix (ECM) production. The aim of this study was to identify NC-secreted substances that stimulate IVD regeneration. By mass spectrometry of porcine, canine and human NCCM, 149, 170 and 217 proteins were identified, respectively, with 66 proteins in common. Mainly ECM-related proteins were identified, but also organelle-derived and membrane-bound vesicle proteins. To determine whether the effect of NCCM was mediated by soluble and/or pelletable factors, porcine and canine NCCM were separated into a soluble (NCCM-S; peptides and proteins) and pelletable (NCCM-P; protein aggregates and extracellular vesicles) fraction by ultracentrifugation, and tested on bovine and canine CLCs *in vitro*, respectively. In each model, NCCM-S exerted a more pronounced anabolic effect than NCCM-P. However, glycosaminoglycan (GAG) uptake from the medium into the carrier gel prevented more definite conclusions. While the effect of porcine NCCM-P on bovine CLCs was negligible, canine NCCM-P appeared to enhance GAG and collagen type II deposition by canine CLCs. In conclusion, porcine and canine NCCM exerted their anabolic effects mainly through soluble factors, but also the pelletable NCCM factors showed moderate regenerative potential. Although the regenerative potential of NCCM-P should not be overlooked, future studies should focus on unraveling the protein-based regenerative mechanism from NCCM produced from isolated NCs, *e.g.* by NCCM fractionation and pathway blocking studies.

Keywords: Intervertebral disc degeneration, nucleus pulposus, notochordal cells, notochordal cell-conditioned medium, proteomics, extracellular vesicles, regenerative medicine, canine, porcine, human.

*Address for correspondence:
Marianna A. Tryfonidou
Department of Clinical Sciences of Companion Animals
Faculty of Veterinary Medicine
Utrecht University
Yalelaan 108
3584 CM Utrecht
the Netherlands

Telephone Number +31-30-2534558
FAX Number: +31-30-25184126
E-mail: m.a.tryfonidou@uu nl

Introduction

Low back pain in humans is associated with intervertebral disc (IVD) degeneration (Cheung *et al.*, 2009; Luoma *et al.*, 2000). The IVD consists of a hydrated nucleus pulposus (NP), mainly composed of proteoglycan (PG) and collagen type II, circumferentially confined by the annulus fibrosus (AF) in which collagen type I is most prominent. The PG's negative charges attract water into the NP, but its swelling is restricted by the AF. This gives rise to high osmotic pressure, crucial for sustaining compressive loads in the healthy IVD. IVD degeneration is a complex, multifactorial process and is characterised by replacement of proteoglycans and collagen type II by a fibrous and dysfunctional tissue high in collagen type I. Current treatment methods aim to alleviate pain without addressing the underlying mechanism of IVD degeneration. Therefore,

cell- or growth factor-based regenerative strategies have gained increased attention (Bach *et al.*, 2014; Benneker *et al.*, 2014; Sakai and Grad, 2015; Sakai and Andersson, 2015). Although several regenerative strategies, *e.g.* allogeneic mesenchymal precursor cell (https://clinicaltrials.gov/ct2/show/NCT01290367)/autologous disc chondrocyte (NCT01640457) transplantation or growth factor application (NCT00813813), have entered the clinical trial phase, no effective regenerative therapy for IVD degeneration is yet clinically available.

In the field of IVD regeneration, notochordal cells (NCs) have gained increasing interest because of their potential regenerative and protective properties (Purmessur *et al.*, 2013). NCs are large, vacuolated cells and are only present in the NP of foetal and young human individuals. They disappear at approximately 10 years of age, leaving the chondrocyte-like cells (CLCs) as the primary cell type in the NP. This process precedes the onset of IVD degeneration, suggesting that NCs play a role in maintaining tissue health. The regenerative effect of NC-secreted factors present in NC-conditioned medium (NCCM) was demonstrated previously on CLCs (Abbott *et al.*, 2012; Potier *et al.*, 2014) and mesenchymal stem cells (MSCs) (de Vries *et al.*, 2015; Korecki *et al.*, 2010; Purmessur *et al.*, 2011), with clear cross-species activity (Bach *et al.*, 2015). Furthermore, porcine NCCM exerted a regenerative effect on bovine NP explants (de Vries *et al.*, 2016), suggesting that NCCM can also stimulate cells in their native tissue.

The use of NCCM itself, however, is not a clinical option; only small volumes can be injected in the IVD, which is likely insufficient to induce a long-term regenerative response. Therefore, identification and subsequent synthetic production of the biologically active factors in NCCM is more appealing. Up to date, only few studies reported on the potential biologically active NCCM factors. Connective tissue growth factor (CTGF) was found in canine (Erwin *et al.*, 2006) and porcine (Gantenbein *et al.*, 2014) NCCM and alpha-2-macroglobulin, clusterin and tenascin were detected in porcine NCCM (Purmessur *et al.*, 2011).

Initial identification of NCCM's active factors has focused on proteomics, but extracellular vesicles (EVs) have not been considered yet. EVs are a heterogeneous group of small, membrane-enclosed particles (~40 nm to ~5 µm), actively released by cells from various tissue types (van der Vlist *et al.*, 2012; Witwer *et al.*, 2013). EVs play an active role in intercellular signalling, since they can express receptor ligands or can be vehicles of signalling molecules. Previous studies indicated that EVs influence various processes, such as pathogenesis of diseases (Anderson *et al.*, 2010) and tissue regeneration (Malda *et al.*, 2016). As such, it was hypothesised that EVs can also be secreted by NCs and may be involved in maintaining healthy NP tissue. The aim of the current study was to identify whether soluble (peptides and proteins) or pelletable (protein aggregates and EVs) factors are responsible for the anabolic effects of NCCM on CLCs. We hypothesised that both the soluble and pelletable factors contribute to the anabolic effects of NCCM.

Materials and Methods

Sources of NC-rich NP tissue and generation of NCCM

Thompson grade I IVDs were collected from 5 porcine, 16 canine and 3 human donors. Porcine spines (3 months of age, C1-S1) were collected from the local abattoir. Canine spines (16-38 months of age, C1-S1) were collected from mixed breed non-chondrodystrophic (NCD) dogs euthanised in unrelated research studies, approved by the Utrecht University Animal Ethics Committee. IVDs from human donors (L2-L5) between 20 weeks of gestation and 2 days of age (postnatal) were obtained during standard *post mortem* diagnostic procedures, approved by the scientific committee of the Pathology Department of the University Medical Centre Utrecht. Anonymous use of redundant tissue for research purposes is a standard treatment agreement with patients in the University Medical Centre Utrecht (Local Medical Ethical Committee (METC) number 12-364). The material was used in line with the code 'Proper Secondary Use of Human Tissue' installed by the Federation of Biomedical Scientific Societies.

Generation of NCCM

Conditioned medium from porcine (n = 5), canine (n = 8) and human (n = 3) NC-rich NP tissue (NCCM+) was generated by culturing NP tissue for 4 d (1 g tissue/30 mL) in hgDMEM+Glutamax (31966, Invitrogen, Paisley, UK) with 1 % penicillin/streptomycin (P11-010, GE Healthcare Life Sciences, Eindhoven, the Netherlands) at 37 °C, 5 % CO_2 and 5 % O_2 (Bach *et al.*, 2015) (Fig. 1**a**). After 4 d, NP tissue was removed and NC-conditioned medium was filtered through 70 µm cell strainers. The filtrate was sequentially centrifuged at 200×*g* and 500×*g* (two times 10 min, 4 °C) to remove (dead) cells and debris. Thereafter, the supernatant (cell-free conditioned medium) was concentrated using a 3 kDa Amicon Ultra-15 Centrifugal filter tube (Merck Millipore, Amsterdam, the Netherlands) at 4000×*g* (45 min, 4 °C). All substances with a molecular weight >3 kDa were resuspended in fresh hgDMEM+Glutamax and stored in aliquots at −70 °C until use. To determine whether the porcine and canine NCCM+ effects were NC-specific, negative control conditioned media (NCCM−) were generated by re-culturing the NP tissue in the presence of 5 % foetal bovine serum (FBS, Gibco 16000-044, Life Technologies, Bleiswijk, the Netherlands); the latter results in loss of vacuolated-NC morphology (Arkesteijn *et al.*, 2013). NP tissue was cultured for 18 d with medium changes twice a week, until no more vacuoles were observed. Subsequently, the NP tissue was washed twice to remove FBS components, and cultured for 4 d in hgDMEM+Glutamax with 1 % P/S to generate NCCM−. NCCM− was centrifuged, filtered and stored similar to NCCM+.

Proteomic analysis of porcine, canine and human NCCM

NCCM+ from 5 porcine, 5 canine and 3 human donors were deglycosylated overnight at 37 °C with 20 U PGNaseF (V4831, Promega, Madison, WI, USA). Protein digestion

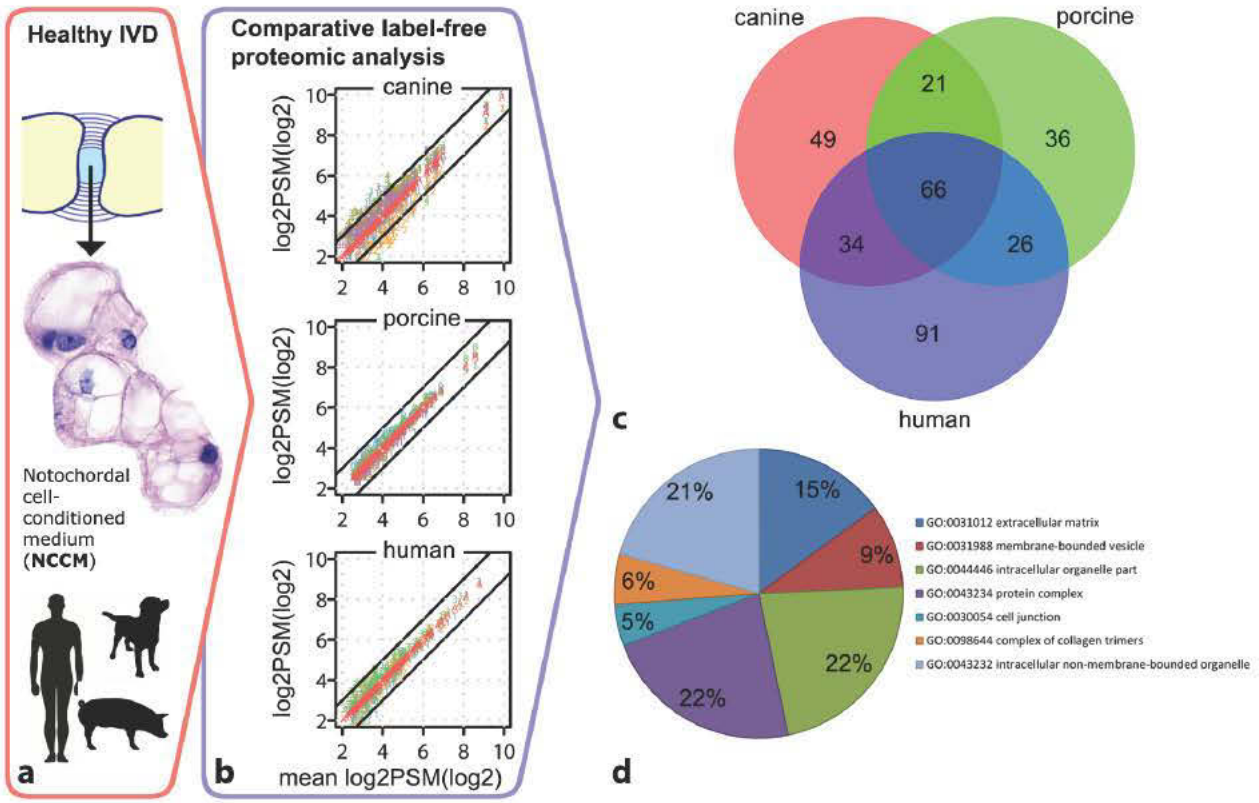

Fig. 1. Proteomic analysis of porcine, canine and human notochordal cell (NC)-conditioned medium (NCCM). (**a**) NCCM was generated from NC-rich nucleus pulposus (NP) tissue of porcine ($n = 5$), canine ($n = 5$) and human ($n = 3$) donors. (**b**) Log2 values of the number of peptide spectrum matches (PSM) plotted against the average number of PSMs for each protein show a higher inter-donor variability for canine NCCM than for porcine and human NCCM. (**c**) The number of proteins discovered in porcine, canine and human NCCM, and their combinations. (**d**) Cell and/or matrix origins of the 66 proteins in common to all three species NCCM.

was performed with filter aided sample preparation (FASP) (Wisniewski *et al.*, 2009) with a buffer containing 8 M urea in 1 mM Tris-HCl at pH 8.0 and pH 8.5; using filters with cut off of 10 kDa (MRCPRT010, YM-10, Microcon, Merck Millipore). Proteins were reduced with 10 mM dithiothreitol (43815, Sigma-Aldrich, Saint Louis, MO, USA), alkylated with 200 mM iodoacetamide (I625-5G, Sigma-Aldrich), and digested first for 4 h with 2 mg/mL LysC (Lysyl Endopeptidase, 129-02541,Wako Chemicals, Richmond, VA, USA) in a ratio of 1:50 and then overnight with 0.1 µg/µL trypsin (V5280, Promega) in a ratio of 1:50. The digested samples were desalted using Oasis HLB 96 well µelution plate (186001828BA, Waters, Etten-Leur, the Netherlands). Finally, samples were dried and reconstituted in 40 µL of 10 % formic acid/5 % dimethyl sulphoxide.

Reversed phase nLC-MSMS analysis was performed using a Proxeon EASY-nLC 1000 (Thermo Scientific, Breda, the Netherlands) (de Graaf *et al.*, 2014). Mass spectra were acquired using a Q-Exactive Plus mass spectrometer (Thermo Scientific) (Marino *et al.*, 2014) at a resolution of 35,000 with a scan range from 375 to 1600 m/z. Dynamic exclusion was set at 10 s. Raw data files were analysed using Proteome Discoverer (version 1.4.1.14, Thermo Scientific) (Marino *et al.*, 2014). Data were searched against the SwissProt version 2014-12 for *Sus scrofa*, *Canis familiaris* or *Homo sapiens*.

Protein profile analysis was performed with R version 3.2.2 (developed by the R Core Team, 2015), using preprocessCore (Bolstad, 2016), biomaRt (Durinck *et al.*, 2009) and VennDiagram (Chen, 2015) packages. For each species, the obtained peptide spectrum match (PSM) values were filtered for each protein on missing or low values. For canine and porcine, the sum of the PSM values for any protein was set at >5 for at least 4 out of 5 samples and for human, the sum was set at >4 for at least 2 out of 3 samples. The PSM values of filtered proteins were log transformed and quantile normalised. Each sample was plotted against the species mean to assess data distribution (Fig. 1). To compare the profiles of the different species, filtered proteins were given a HGNC gene name using the Uniprot, Ensembl and HGNC databases and annotation results were manually curated. Per species, gene name lists were compared using a venn diagram and the different overlapping sets were analysed using toppgene (ToppFun) analysis (Chen *et al.*, 2009). Enriched GO Cellular Component terms were remapped to common ancestors within the GO Cellular Component term using GO.db version 3.2.2 (Carlson, 2016).

Separation of the soluble and pelletable NCCM fraction

To unravel whether the biologically active factors in NCCM+ were present in the soluble (NCCM-S) or pelletable (NCCM-P) fraction, ultracentrifugation was performed (van der Vlist *et al.*, 2012). 37 mL porcine or canine NCCM was ultracentrifuged at 10,000×*g* (30 min,

8,700 rpm; RCF average 10,016×*g*; RCF max 13,648×*g*; κ-factor 2543.1) and 100,000×*g* (65 min, 23,000 rpm; RCF average 70,002×*g*; RCF max 95,389×*g*; κ-factor 363.9) at 4 °C (Beckman Coulter Optima L-90K ultracentrifuge, SW28 rotor). After 100,000×*g* ultracentrifugation, the supernatant containing soluble factors (NCCM-S) was aliquoted and stored at −70 °C until use. The 100,000×*g* pellet, containing EVs and protein aggregates, was suspended in 246 µL phosphate-buffered saline (PBS) supplemented with 0.2 % EV-free bovine serum albumin (BSA, A9418, Sigma-Aldrich) (6.7 µL PBS/0.2 % BSA per mL NCCM) and stored at −70 °C until use. The PBS/0.2 % BSA was depleted from EVs by ultracentrifugation overnight at 100,000×*g*. Directly prior to use for culture, aliquots of the pelletable factors (dissolved in PBS/0.2 % BSA) were thawed rapidly for maximal functional preservation (Witwer *et al.*, 2013). Thereafter, in order to yield NCCM-P, 6.7 µL of the 100,000×*g* pellet was added to 1 mL basal culture medium (hgDMEM+Glutamax with 1 % P/S, 1 % ITS+ premix (354352, Corning Life Sciences, Amsterdam, the Netherlands), 0.04 mg/mL L-proline (P5607, Sigma-Aldrich), 0.1 mM ascorbic acid 2-phosphate, and 1.25 mg/mL BSA. The EV content of NCCM-P was hereby similar to NCCM+.

Biochemical analysis of NCCM and its fractions

The protein concentration of NCCM+, NCCM−, NCCM-S and NCCM-P (porcine $n = 4$, canine $n = 8$) was assessed using the Qubit® Protein Assay Kit (Q33211, Invitrogen) according to the manufacturer's instructions. In addition, a dimethyl methylene blue (DMMB) assay (Farndale *et al.*, 1982) was performed to determine the glycosaminoglycan (GAG) concentration.

***In vitro* culture of bovine and canine CLCs in pelletable and soluble fractions of NCCM**

Bovine CLCs ($n = 4$ repeats, CLCs from 2 donors pooled per repeat, 2-2.5 years of age, Thompson grade II) were harvested from caudal IVDs obtained from the local abattoir, and chondrodystrophic (CD) canine CLCs ($n = 4$, 3-10 years of age, Thompson grade III) were harvested from IVDs of dogs euthanised in unrelated research studies, approved by the Utrecht University Animal Ethics Committee. NPs were enzymatically digested with 0.1 % pronase (10165921001, Roche Diagnostics, Almere, the Netherlands) for 90 min and subsequently with 0.025 % collagenase type II (LS004177, Worthington, Lakewood, NJ, USA) for 16 h at 37 °C.

Bovine CLCs were suspended in 1.2 % alginate (180947, Sigma-Aldrich) beads of approximately 20 µL at 3 × 10^6 cells/mL (Guo *et al.*, 1989). Empty (no cell-containing) and CLC-containing beads were cultured for 28 d at 37 °C, 5 % CO_2 and 5 % O_2 in basal medium or in porcine NCCM+, NCCM−, NCCM-S or NCCM-P (four different porcine NCCM donors), each with the same supplements as basal culture medium.

Given that canine CLCs did not thrive in alginate beads (Arkesteijn *et al.*, 2015), an albumin-based hydrogel was used (Scholz *et al.*, 2010). Canine CLCs from four donors were pooled to assess the effect of donor-specific NCCM on a representative canine CLC population. Passage 2 CLCs were incorporated in 40 µL hydrogels composed of chemically activated albumin cross-linked by polyethylene glycol spacers (Benz *et al.*, 2012) (3 × 10^6 cells/mL hydrogel). The albumin- and hyaluronic acid-containing hydrogels were cultured for 28 d at 37 °C, 5 % CO_2 and 5 % O_2 in basal culture medium with/without 10 ng/mL transforming growth factor-β_1 (TGF-β_1, 240-B, R&D Systems, Minneapolis, MN, USA), or in canine NCCM+, NCCM−, NCCM-S or NCCM-P (eight different canine NCCM donors), each with the same supplements as basal medium. Unlike bovine CLCs, canine CLCs do not produce a considerable amount of GAGs if no growth factor is supplemented to the culture medium. Therefore, a positive control (10 ng/mL TGF-β_1) was used to show that the canine CLC donors were able to produce GAGs if a proper stimulus was provided, *e.g.* in case these donors would not respond to NCCM. Since the hydrogel bound GAGs present in NCCM, empty hydrogels were cultured along for each NCCM−/NCCM+/NCCM-S/NCCM-P donor to be able to correct for this.

Gene expression profiling (RT-qPCR; canine $n = 8$) was performed at day 4, the DNA content (dsDNA High Sensitivity Assay Kit, Q32851, Invitrogen) and GAG content (DMMB assay; porcine NCCM-treated bovine CLCs $n = 4$ and canine NCCM-treated canine CLCs $n = 8$ *in duplo*) were determined at days 0 and 28, and Safranin O/Fast Green staining and collagen type I and II immunohistochemistry (porcine NCCM-treated bovine CLCs $n = 3$-4 and canine NCCM-treated canine CLCs $n = 4$-8) were performed at day 28 (Bach *et al.*, 2015). For gene expression profiling, four reference genes (*GAPDH*, *HPRT*, *RPS19* and *SDHA*) were chosen to normalise gene expression of the target genes *ACAN*, *ADAMTS5*, *BAX*, *BCL-2*, *CASP3*, *COL1A1*, *COL2A1*, *COL10A1*, *CCND1*, *FOXF1, KRT8, KRT18, KRT19, MMP13, T* and *VEGF*. Primer sequences are depicted in Table 1. The DMMB assay was done with the following modifications: papain and DMMB solution pH was adjusted to 6.8 and guanidinium chloride was used to mask hyaluronic acid.

Testing fresh *versus* frozen pelletable NCCM factors *in vitro*

To determine whether freezing the pelletable factors affected their biological effect, micro-aggregates of 35,000 CD canine CLCs were generated (Bach *et al.*, 2015). CLCs have more easy access to the pelletable factors in this culture model compared with hydrogels. The micro-aggregates were cultured in low-adherence 96-well plates (650970, CELLSTAR®, Greiner Bio-one, Alphen a/d Rijn, the Netherlands) at 37 °C, 5 % CO_2 and 5 % O_2 for 7 d and were treated with basal culture medium (control), freshly generated, non-frozen NCCM-P (P1x fresh; kept at 4 °C for maximum 4 d) or canine NCCM-P that was frozen at −70 °C for maximum 4 d (P1x frozen). To determine whether a higher concentration pelletable factors would exert a more pronounced effect, fresh and frozen pelletable factors were also applied in a 10× higher concentration than present in NCCM+ (NCCM-P10× fresh and NCCM-P10× frozen, respectively). The same CD canine CLC donors as used in the hydrogel experiment and 4 different NCD canine NCCM donors were used for

Table 1. Primers used for quantitative PCR of canine samples.

Genes	Forward sequence 5' → 3'	Reverse sequence 5' → 3'	Amplicon size	Annealing temp (°C)	Accession no.
Reference genes					
GAPDH	TGTCCCCACCCCCAATGTATC	CTCCGATGCCTGCTTCACTACCTT	100	58	NM_001003142
HPRT	AGCTTGCTGGTGAAAAGGAC	TTATAGTCAAGGGCATATCC	104	58	NM_001003357
RPS19	CCTTCCTCAAAAAGTCTGGG	GTTCTCATCGTAGGGAGCAAG	95	61	XM_005616513
SDHA	GCCTTGGATCTCTTGATGGA	TTCTTGGCTCTTATGCGATG	92	56.5	XM_535807
Target genes					
ACAN	GGACACTCCTTGCAATTTGAG	GTCATTCCACTCTCCCTTCTC	111	62	XM_005618252
ADAMTS5	CTACTGCACAGGGAAGAG	GAACCCATTCCACAAATGTC	149	61	XM_846025.3
BAX	CCTTTTGCTTCAGGGTTTCA	CTCAGCTTCTTGGTGGATGC	108	58	NM_001003011.1
BCL2	TGGAGAGVGTCAACCGGGAGATGT	AGGTGTGCAGATGCCGGTTCAGGT	87	62	NM_001002949
CASP3	ATCACTGAAGATGGATGGGTTGGGTT	TGAAAGGAGCATGTTCTGAAGTAGCACT	139	58	NM_001003042
COL1A1	GTGTGTACAGAACGGCCTCA	TCGCAAATCACGTCATCG	109	61	NM_001003090
COL2A1	GCAGCAAGAGCAAGGAC	TTCTGAGAGCCCTCGGT	151	62	XM_005636674
COL10A1	CCAACACCAAGACACAG	CAGGAATACCTTGCTCTC	80	61	XM_003639401.2
CCND1	GCCTCGAAGATGAAGGAGAC	CAGTTTGTTCACCAGGAGCA	117	60	NM_001005757.1
FOXF1	GAGTTCGTCTTCTCCTTCAACAC	GCTTGATGTCTTGGTAGGTGAC	99	60	XM_546792.5
KRT8	CCTTAGGCGGGTCTCTCGTA	GGGAAGCTGGTGTCTGAGTC	149	63	XM_543639
KRT18	GGACAGCTCTGACTCCAGGT	AGCTTGGAGAACAGCCTGAG	97	60	XM_534794
KRT19	GCCCAGCTGAGCGATGTGC	TGCTCCAGCCGTGACTTGATGT	86	64	NM_001253742
MMP13	CTGAGGAAGACTTCCAGCTT	TTGGACCACTTGAGAGTTCG	250	65	XM_536598
T	AGACAGCCAGCAATCTG	TGGAGGGAAGTGAGAGG	115	53	NM_001003092.1
VEGF	CTTTCTGCTCTCCTGGGTGC	GGTTTGTGCTCTCCTCCTGC	101	58	NM_001003175

All primers were designed in-house using Perlprimer except for *MMP13* (Muir *et al.*, 2005) and *BAX* (Mahmoudabady *et al.*, 2013). **Abbreviations used**: *GAPDH*, glyceraldehyde 3-phosphate dehydrogenase; *HPRT*, hypoxanthine-guanine phosphoribosyltransferase; RPS19, ribosomal protein S19; *SDHA*, succinate dehydrogenase subunit A; *ACAN*, aggrecan, *ADAMTS5*, a disintegrin and metalloproteinase with thrombospondin motifs 5; *BAX*, Bcl2-like-protein; *BCL-2*, B-cell CLL/lymphoma 2; *CASP3*, caspase-3; *COL1A1*, collagen type I; *COL2A1*, collagen type II; *COL10A1*, collagen type X; *CCND1*, cyclin D1; *FOXF1*, forkhead box F1; *KRT8*, keratin 8; *KRT18*, keratin 1; *KRT19*, keratin 19; *MMP13*, matrix metalloproteinase 13; *T*, brachyury; *VEGF*, vascular endothelial growth factor.

this part of the study. Gene expression profiling (RT-qPCR; $n = 8$) was performed at day 4 and the DNA and GAG contents of the micro-aggregates ($n = 8$) were determined at day 7 as described above.

Statistical analysis of cell culture experiments

Statistical analyses were performed using IBM SPSS statistics 22. Data were examined for normal distribution using a Shapiro Wilks test. Kruskal Wallis and Mann-Whitney U test were performed on non-normally distributed data and one-way ANOVA on normally distributed data. Benjamini & Hochberg False Discovery Rate *post-hoc* tests were performed to correct for multiple comparisons. In all tests, a p-value < 0.05 was considered significant.

Results

Proteomic analysis of porcine, canine and human NCCM+

NCCM+ from 5 porcine, 5 canine and 3 human donors was subjected to mass spectrometry and bioinformatic analysis. Log2-values of the number of PSMs plotted against the log2-values of the mean PSM number for each protein showed a wider distribution for canine NCCM, indicating a higher inter-donor variability than porcine and human NCCM (Fig. 1**b**). Raw pre-filtered protein profiles for porcine, canine and human NCCM contained, respectively, 737, 847 and 779 Uniprotids of which 153, 178 and 217 were left after filtering. These were annotated to 149, 170 and 217 different HGNC gene names for porcine, canine and human, respectively, and were used for profile comparisons (Table 2). The three species had 66 of these proteins in common. A large fraction of the proteins was derived from organelles (22 %, Fig. 1) and macromolecular protein complexes (24 %). Furthermore, a considerable amount of extracellular matrix (ECM) (16 %) and membrane-bound vesicle proteins (10 %) were found in NCCM from all species.

Pathway analysis (Reactome, V55) of all common proteins revealed various processes involved in ECM and its structure (Table 3). The GAG-, collagen-, hyaluronic acid- and integrin-binding pathways were significantly covered, as well as the structural molecule activity and protein complex binding pathways. Other detected pathways contained growth factor- and enzyme-binding proteins.

Due to the presence of specific collagens (*e.g.* types III, V and XV) in porcine and human, but not in canine NCCM, pathways involved in the assembly of collagen fibrils, biosynthesis and formation were significantly covered

Table 2. Proteins identified in canine, porcine and human NCCM.

Canine	Porcine	Human	Number	Proteins
Yes	Yes	Yes	66	ACAN, FN1, KRT8, COMP, COL6A3, CA3, ALB, VIM, CLU, KRT19, A2M, HSPG2, CHAD, ABI3BP, XYLT1, ENO1, KRT18, CILP, PKM, COL6A1, COL2A1, EFEMP1, LAMB2, HAPLN1, ACTN4, CLEC3A, RNASE4, TPI1, ACTN1, ACTC1, EHD2, LMNA, LAMA4, SERPINE2, CILP2, PRELP, LAMC1, CSPG4, COL11A2, HTRA1, CD109, LDHA, ENO3, VCAN, HBB, NID2, QSOX1, PRDX1, ANXA2, LGALS1, FMOD, KRT15, UGP2, PRDX6, PEBP1, YWHAE, YWHAZ, EEF1A1, TUBB4B, RARRES2, THBS4, CHRDL2, ALDOC, PLOD1, MATN2, YWHAG
No	Yes	Yes	26	AEBP1, ANXA1, ANXA5, ACTB, CLEC3B, COL11A1, COL15A1, COL3A1, COL5A1, COL5A2, COL6A2, DPYSL2, EZR, GDI1, FBLN7, MSN, PCOLCE, PFN1, PGAM1, PPIA, PYGL, SERPINB1, SERPINF1, SOD1, TNXB, VCL
Yes	No	Yes	34	TF, APOE, GAPDH, TNC, SERPINA1, SPTAN1, PGK1, GPI, LUM, LYZ, PRG4, DCN, ENO2, ALDOA, SERPINA3, HBA1, GSN, EDIL3, MFGE8, HIST4H4, LGALS3, FBLN1, HSPA8, DES, BGN, SPARC, TGFBI, HSP90AA1, CLSTN1, MDH1, CFH, FRZB, TKT, YWHAB
No	No	Yes	91	COL14A1, COL12A1, THBS1, HBG2, HBG1, PDIA3, IGHG1, THBS3, C4B, PPIB, POTEE, RNASE1, MATN4, CALM1, COL9A1, COL1A1, OGN, SSC5D, IGKC, KRT1, PRDX2, COL1A2, HBD, MATN3, P4HB, CFD, MMP3, EMILIN1, ANG, NUCB1, CAPG, C1S, ACTBL2, IGHG3, SPTBN1, FABP4, ITIH5, COL16A1, APOH, UBC, YWHAQ, IGHG2, C1R, IGHG4, LOXL2, VIT, B2M, CKM, ECM1, SERPINA5, KRT10, TUBA1B, FGFBP2, FBN1, DBI, PRDX4, TUBB2A, CLEC11A, RCN1, GSTP1, HSPA1B, CA1, FNDC1, KRT7, HNRNPA2B1, HNRNPA1, C3, KRT9, SELENBP1, FSTL1, HAPLN3, PGM1, FGA, FABP5, CALU, SLPI, HSP90B1, IQGAP1, TP53I3, RCN3, FBLN2, FLNA, MXRA5, TMSB4X, S100A10, CAT, HSP90AB1, DSC3, FSCN1, LRP1, CYCS
Yes	Yes	No	21	SEMA3C, ENPP2, CP, CCL16, PCOLCE2, CCDC80, unchar1, APP, THY1, EHD3, KRT75, KRT14, SMOC1, ACTN2, TPM1, LECT2, unchar2, HSPA2, TUBB, TUBB2B, TIMP2
No	Yes	No	36	AHNAK, ANXA8, LOC100157318, CFB, SERPING1, C4A, CAPN2, CHADL, CHI3L1, FLNC, HBQ1, H2BFS, HSPB1, KRT5, LOC100626701, ORM1, HIST2HBE, LOC102164134, LOC100524210, MFI2, MYH9, NME2, NPEPPS, PFKL, PRKCDBP, RDX, LOC100736872, SERPINA3-3, SPARCL1, SPP1, LOC100049693, TPM4, VAT1, SEMA7A, unchar3, H3F3A
Yes	No	No	49	CDH1, SLIT3, OLFML2B, PGAM4, CA2, KRT13, LGALS3BP, SOD3, ANOS1, LOC477441, MB, MRC2, LTF, col11a2, MFAP4, TNFRSF11B, HSPA1A, LOC100855540, LDHB, NCAM1, CHST3, LOC476825, LOXL3, KRT17, LOC100855471, TIMP3, CRYAB, CKB, SEMA3E, CFL1, LOC488254, HSPA5, CCL21, HIST1H2AH, PTRF, CSTB, LECT1, CHST6, PGAM2, TUBA1A, SLC2A1, TUBB4A, CDH2, HIST1H1C, FHL1, SDCBP, KRT78, GSTM3, EFEMP2

by proteins present in human and porcine NCCM (Table 4). Also, proteins from platelet-involved pathways were found in these two species (Table 4). Analysis of proteins common in human and canine NCCM demonstrated pathways related to glucose metabolism (Table 5). Furthermore, due to the presence of decorin and biglycan, dermatan sulphate and chondroitin sulphate biosynthesis pathways were significantly covered in human and canine NCCM (Table 5). Both canine and porcine NCCM (Table 6) contained proteins involving tubulin-related pathways. Furthermore, several pathways with proteins present in only human, porcine or canine NCCM were detected (Tables 7-9). In porcine (Table 7) and human NCCM (Table 9), proteins related to complement binding pathways were detected. Lastly, proteins from axon guidance-related pathways were present in NCCM from all species (Tables 4 and 8).

A significant number of proteins involved with transcription factor (*e.g.* activator protein 1 (AP-1) and paired box gene 4 (PAX4)) binding sites were found in NCCM from all species (Table 10). Furthermore, proteins (predicted to be) targeted by miRNA29 were found in human and porcine NCCM (Table 11).

In vitro culture of bovine CLCs in porcine NCCM

Porcine NCCM and its fractions were analysed for their protein and GAG concentration (Fig. 2**a**). NCCM-S contained a similar protein concentration as NCCM+, whereas the protein concentration of NCCM-P was significantly lower than that of NCCM+, NCCM-S and NCCM− ($p < 0.05$). The NCCM− protein concentration was significantly lower than that of NCCM+ ($p < 0.05$). Also the GAG concentration of NCCM+ and NCCM-S was comparable, and both were significantly higher than that of NCCM-P and NCCM− ($p < 0.05$). Although few GAGs were present in NCCM−, its GAG concentration was still significantly higher than that of NCCM-P ($p < 0.05$).

After 28 d, bovine CLC-containing alginate beads cultured in porcine NCCM (fractions) were analysed for DNA and GAG content and histology and compared with controls. Empty alginate beads did not bind GAGs (not shown). Although CLCs proliferated and formed clusters in all conditions, no statistically significant differences in DNA content were found between conditions (Fig. 2**b**). The GAG and GAG/DNA content was, however, significantly increased for culture in NCCM+ and NCCM-S compared to control medium ($p < 0.05$), whereas it was not increased for NCCM− or NCCM-P (Fig. 2**c** and 2**d**). The increased GAG content in NCCM+ and NCCM-S-treated beads was confirmed by Safranin O/Fast Green staining (Fig. 2**e**). Immunohistochemical staining showed no collagen type I deposition in any condition. Collagen type II, however, was deposited in all conditions: only in the pericellular region in the control- and NCCM-P-treated alginate beads, but more abundant after NCCM+, NCCM-S and NCCM− treatment.

In vitro culture of canine CLCs in canine NCCM

Canine NCCM and its fractions were analysed for their protein and GAG concentration (Fig. 3**a**). The protein and

Table 3. Gene onthology analysis of proteins identified in porcine, canine and human NCCM.

Rank	GO term	Name	q-value FDR B&H	Hit Count in Query List	Hit Count in Genome	Hit in Query List
1	GO:0005539	Glycosaminoglycan binding	7.96E-08	11	216	THBS4, SERPINE2, ANG, FMOD, FN1, COMP, ABI3BP, PRELP, ACAN, VCAN, HAPLN1
2	GO:0005201	Extracellular matrix structural constituent	8.35E-07	7	70	COL2A1, COL11A2, COMP, PRELP, ACAN, LAMA4, LAMC1
3	GO:0005198	Structural molecule activity	4.30E-06	15	748	COL2A1, VIM, TUBB4B, KRT8, COL11A2, KRT15, COMP, LMNA, KRT18, KRT19, PRELP, ACAN, LAMA4, LAMB2, LAMC1
4	GO:0008201	Heparin binding	9.30E-06	8	164	THBS4, SERPINE2, ANG, FMOD, FN1, COMP, ABI3BP, PRELP
5	GO:0005518	Collagen binding	1.23E-05	6	71	NID2, THBS4, FN1, COMP, ABI3BP, CSPG4
6	GO:0032403	Protein complex binding	1.48E-04	15	1053	VIM, NID2, KRT8, THBS4, FN1, COMP, ABI3BP, KRT19, CSPG4, PKM, LAMB2, ACTN4, ACTN1, YWHAE, YWHAZ
7	GO:1901681	Sulphur compound binding	1.48E-04	8	257	THBS4, SERPINE2, ANG, FMOD, FN1, COMP, ABI3BP, PRELP
8	GO:0019899	Enzyme binding	1.48E-04	20	1851	A2M, VIM, HSPG2, FN1, COMP, LMNA, CLU, PEBP1, ANXA2, VCAN, CSPG4, ALB, LDHA, ENO1, YWHAE, YWHAG, YWHAZ, PRDX6, EEF1A1, TPI1
9	GO:0004867	Serine-type endopeptidase inhibitor activity	8.34E-04	5	96	A2M, COL6A3, SERPINE2, PEBP1, CD109
10	GO:0097110	Scaffold protein binding	1.51E-03	4	56	VIM, KRT8, KRT15, KRT18
11	GO:0002020	Protease binding	1.63E-03	5	115	A2M, HSPG2, FN1, COMP, ANXA2
12	GO:0005178	Integrin binding	1.69E-03	5	118	THBS4, FN1, LAMB2, ACTN4, ACTN1
13	GO:0004857	Enzyme inhibitor activity	1.74E-03	8	393	A2M, COL6A3, SERPINE2, PEBP1, ANXA2, CD109, CHAD, YWHAG
14	GO:0004634	Phosphopyruvate hydratase activity	1.74E-03	2	4	ENO1, ENO3
15	GO:0005540	Hyaluronic acid binding	1.79E-03	3	24	ACAN, VCAN, HAPLN1
16	GO:0019838	Growth factor binding	2.28E-03	5	134	COL2A1, A2M, COL6A1, HTRA1, CD109
17	GO:0003723	RNA binding	2.28E-03	16	1608	VIM, TUBB4B, ANG, KRT18, PEBP1, ANXA2, PRDX1, PKM, ACTN4, ACTN1, ENO1, YWHAE, YWHAG, YWHAZ, LGALS1, EEF1A1
18	GO:0061134	Peptidase regulator activity	2.39E-03	6	221	A2M, COL6A3, SERPINE2, FN1, PEBP1, CD109
19	GO:0016209	Antioxidant activity	2.51E-03	4	75	PRDX1, ALB, HBB, PRDX6
20	GO:0005509	Calcium ion binding	2.54E-03	10	694	NID2, THBS4, EFEMP1, COMP, ANXA2, MATN2, VCAN, ACTN4, ACTN1, EHD2

Table 4. Pathway analysis of proteins identified in porcine and human NCCM.

Rank	ID	Name	q-value FDR B&H	Hit Count in Query List	Hit Count in Genome	Hit in Query List
1	730306	Assembly of collagen fibrils and other multimeric structures	5.9E-09	7	54	COL3A1, COL5A1, COL5A2, COL6A2, COL11A1, COL15A1, PCOLCE
2	645289	Collagen biosynthesis and modifying enzymes	1.1E-08	7	65	COL3A1, COL5A1, COL5A2, COL6A2, COL11A1, COL15A1, PCOLCE
3	645288	Collagen formation	3.5E-08	7	87	COL3A1, COL5A1, COL5A2, COL6A2, COL11A1, COL15A1, PCOLCE
4	576262	Extracellular matrix organization	1.9E-06	8	264	COL3A1, COL5A1, COL5A2, COL6A2, COL11A1, COL15A1, TNXB, PCOLCE
5	161004	Recycling pathway of L1	4.5E-04	3	27	EZR, DPYSL2, MSN
6	106050	Platelet degranulation	5.6E-04	4	85	PFN1, PPIA, VCL, SOD1
7	106048	Response to elevated platelet cytosolic Ca2+	6.5E-04	4	90	PFN1, PPIA, VCL, SOD1
8	105688	Axon guidance	3.0E-03	5	262	EZR, COL6A2, DPYSL2, PFN1, MSN
9	161003	L1CAM interactions	1.1E-02	3	94	EZR, DPYSL2, MSN
10	106034	Platelet activation, signalling and aggregation	1.1E-02	4	214	PFN1, PPIA, VCL, SOD1

Table 5. Pathway analysis of proteins identified in canine and human NCCM.

Rank	ID	Name	q-value FDR B&H	Hit Count in Query List	Hit Count in Genome	Hit in Query List
1	106204	Gluconeogenesis	2.1E-07	6	33	GPI,MDH1, ALDOA, GAPDH, ENO2, PGK1
2	105911	Glycolysis	1.5E-06	5	29	GPI, ALDOA, GAPDH, ENO2, PGK1
3	106196	Metabolism of carbohydrates	3.3E-06	9	266	GPI, LUM, MDH1, DCN, ALDOA, GAPDH, ENO2, PGK1, BGN
4	106199	Glucose metabolism	3.9E-06	6	75	GPI, MDH1, ALDOA, GAPDH, ENO2, PGK1
5	833812	ECM proteoglycans	1.5E-05	5	55	SPARC, LUM, DCN, TNC, BGN
6	366238	Amyloids	1.0E-04	5	85	TGFBI, MFGE8, LYZ, HIST1H4A, GSN
7	576262	Extracellular matrix organization	2.1E-04	7	264	FBLN1, SPARC, LUM, DCN, TNC, BGN, DDR2
8	771599	Binding and uptake of ligands by scavenger receptors	4.9E-04	4	61	SPARC, APOE, HBA1, HSP90AA1
9	530764	Disease	3.1E-03	11	1088	TGFBI, MFGE8, APOE, LUM, DCN, LYZ, HIST1H4A, YWHAB, GSN, HSP90AA1, BGN
10	645310	Dermatan sulphate biosynthesis	6.0E-03	2	11	DCN, BGN
11	105679	Caspase-mediated cleavage of cytoskeletal proteins	7.0E-03	2	12	SPTAN1, GSN
12	645311	CS/DS degradation	8.9E-03	2	14	DCN, BGN
13	477135	Metabolism	1.5E-02	12	1575	GPI, APOE, LUM, MDH1, HBA1, DCN, ALDOA, GAPDH, ENO2, PGK1, HSP90AA1, BGN
14	645309	Chondroitin sulphate biosynthesis	1.8E-02	2	21	DCN, BGN
15	106050	Platelet degranulation	2.0E-02	3	85	SERPINA1, SPARC, ALDOA
16	106048	Response to elevated platelet cytosolic Ca2+	2.3E-02	3	90	SERPINA1, SPARC, ALDOA
17	645305	A tetrasaccharide linker sequence is required for GAG synthesis	2.5E-02	2	26	DCN, BGN
18	685546	MPS VII - Sly syndrome	3.7E-02	3	121	LUM, DCN, BGN
19	685536	Mucopolysaccharidoses	3.7E-02	3	121	LUM, DCN, BGN
20	685547	MPS IX - Natowicz syndrome	3.7E-02	3	121	LUM, DCN, BGN

Table 6. Pathway analysis of proteins identified in porcine and canine NCCM.

Rank	ID	Name	q-value FDR B&H	Hit Count in Query List	Hit Count in Genome	Hit in Query List
1	106248	Post-chaperonin tubulin folding pathway	2.88E-02	2	19	TUBB2A, TUBB2B
2	106245	Formation of tubulin folding intermediates by CCT/TriC	2.88E-02	2	22	TUBB2A, TUBB2B
3	106244	Prefoldin mediated transfer of substrate to CCT/TriC	2.88E-02	2	28	TUBB2A, TUBB2B
4	106243	Cooperation of prefoldin and TriC/CCT in actin and tubulin folding	2.88E-02	2	29	TUBB2A, TUBB2B
5	106262	Striated muscle contraction	2.88E-02	2	31	TPM1, ACTN2
6	106242	Chaperonin-mediated protein folding	4.66E-02	2	50	TUBB2A, TUBB2B
7	106261	Muscle contraction	4.66E-02	2	51	TPM1, ACTN2
8	106241	Protein folding	4.66E-02	2	55	TUBB2A, TUBB2B

Table 7. Pathway analysis of proteins identified only in porcine NCCM.

Rank	ID	Name	q-value FDR B&H	Hit Count in Query List	Hit Count in Genome	Hit in Query List
1	106412	Activation of C3 and C5	0.00829	2	5	C4A, CFB
2	576254	Regulation of complement cascade	0.04694	2	22	C4A, CFB

Table 8. Pathway analysis of proteins identified only in canine NCCM.

Rank	ID	Name	q-value FDR B&H	Hit Count in Query List	Hit Count in Genome	Hit in Query List
1	576262	Extracellular matrix organization	0.02383	6	264	MFAP4, COL11A2, EFEMP2, NCAM1, LOXL3, CDH1
2	730310	Elastic fibre formation	0.02651	3	41	MFAP4, EFEMP2, LOXL3
3	106248	Post-chaperonin tubulin folding pathway	0.04144	2	19	TUBB4A, TUBA1A
4	105688	Axon guidance	0.04144	5	262	CFL1, SLIT3, NCAM1, SDCBP, SEMA3E
5	106245	Formation of tubulin folding intermediates by CCT/TriC	0.04565	2	22	TUBB4A, TUBA1A

Table 9. Pathway analysis of proteins identified only in human NCCM.

Rank	ID	Name	q-value FDR B&H	Hit Count in Query List	Hit Count in Genome	Hit in Query List
1	106406	Initial triggering of complement	4.93E-09	9	40	CFD, IGHG1, IGHG2, IGHG3, IGHG4, IGKC, C1R, C1S, C3
2	576262	Extracellular matrix organization	2.82E-08	16	264	THBS1, COL9A1, COL12A1, FBLN2, FBN1, COL16A1, P4HB, LOXL2, MATN3, FGA, COL14A1, MATN4, MMP3, PPIB, COL1A1, COL1A2
3	106405	Complement cascade	6.88E-08	9	58	CFD, IGHG1, IGHG2, IGHG3, IGHG4, IGKC, C1R, C1S, C3
4	645288	Collagen formation	1.23E-07	10	87	COL9A1, COL12A1, COL16A1, P4HB, LOXL2, COL14A1, MMP3, PPIB, COL1A1, COL1A2
5	106409	Classical antibody-mediated complement activation	1.35E-07	7	28	IGHG1, IGHG2, IGHG3, IGHG4, IGKC, C1R, C1S
6	106407	Creation of C4 and C2 activators	5.19E-07	7	34	IGHG1, IGHG2, IGHG3, IGHG4, IGKC, C1R, C1S
7	645289	Collagen biosynthesis and modifying enzymes	2.26E-06	8	65	COL9A1, COL12A1, COL16A1, P4HB, COL14A1, PPIB, COL1A1, COL1A2
8	106050	Platelet degranulation	1.86E-04	7	85	CFD, FLNA, THBS1, CALM2, CALU, FGA, TMSB4X
9	106048	Response to elevated platelet cytosolic Ca2+	2.35E-04	7	90	CFD, FLNA, THBS1, CALM2, CALU, FGA, TMSB4X
10	771578	FCGR activation	2.35E-04	5	34	IGHG1, IGHG2, IGHG3, IGHG4, IGKC
11	771599	Binding and uptake of ligands by scavenger receptors	2.70E-04	6	61	HSP90B1, IGKC, LRP1, HBD, COL1A1, COL1A2
12	730309	Collagen degradation	3.54E-04	5	38	COL9A1, COL12A1, COL16A1, COL14A1, MMP3
13	771580	Role of phospholipids in phagocytosis	8.80E-04	5	46	IGHG1, IGHG2, IGHG3, IGHG4, IGKC
14	771579	Regulation of actin dynamics for phagocytic cup formation	1.16E-03	6	81	IGHG1, IGHG2, IGHG3, IGHG4, IGKC, HSP90AB1
15	106110	Integrin cell surface interactions	4.22E-03	5	66	THBS1, COL9A1, FBN1, COL16A1, FGA
16	771577	Fcgamma receptor (FCGR) dependent phagocytosis	4.22E-03	6	105	IGHG1, IGHG2, IGHG3, IGHG4, IGKC, HSP90AB1
17	106410	Alternative complement activation	9.39E-03	2	4	CFD, C3
18	833814	Scavenging by class A receptors	1.01E-02	3	19	HSP90B1, COL1A1, COL1A2
19	576263	Degradation of the extracellular matrix	1.42E-02	5	89	COL9A1, COL12A1, COL16A1, COL14A1, MMP3
20	730306	Assembly of collagen fibrils and other multimeric structures	1.74E-02	4	54	LOXL2, MMP3, COL1A1, COL1A2

Table 10. Proteins associated with transcription factor binding sites in porcine, canine and human NCCM.

Venn-group	ID	q-value FDR B&H	Hit Count in Query List	Hit Count in Genome	Hit in Query List
Common	TGANTCA_V$AP1_C	1.63E-02	15	919	XYLT1, HSPG2, KRT8, KRT15, KRT19, CSPG4, PKM, LAMC1, ACTN4, ENO1, ENO3, YWHAG, YWHAZ, LGALS1, EEF1A1
Common	GGGTGGRR_V$PAX4_03	4.51E-02	15	1068	A2M, VIM, HSPG2, NID2, COL6A3, COL11A2, RARRES2, PRELP, CD109, LAMB2, YWHAE, YWHAG, YWHAZ, EEF1A1, HAPLN1
Canine and porcine	TATAAA_V$TATA_01	2.49E-02	7	1075	CP,LECT2, SEMA3C, ENPP2, KRT14, ACTN2, SMOC1
Canine	V$ZIC3_01	3.55E-02	6	213	CRYAB, TIMP3, EFEMP2, SLIT3, LOXL3, CHST3
Canine	GGGAGGRR_V$MAZ_Q6	3.55E-02	17	1838	TUBB4A, KRT13, COL11A2, KRT17, MRC2, CFL1, LECT1, EFEMP2, SLIT3, CHST6, NCAM1, PTRF, LOXL3, CDH2, LDHB, SLC2A1, SOD3

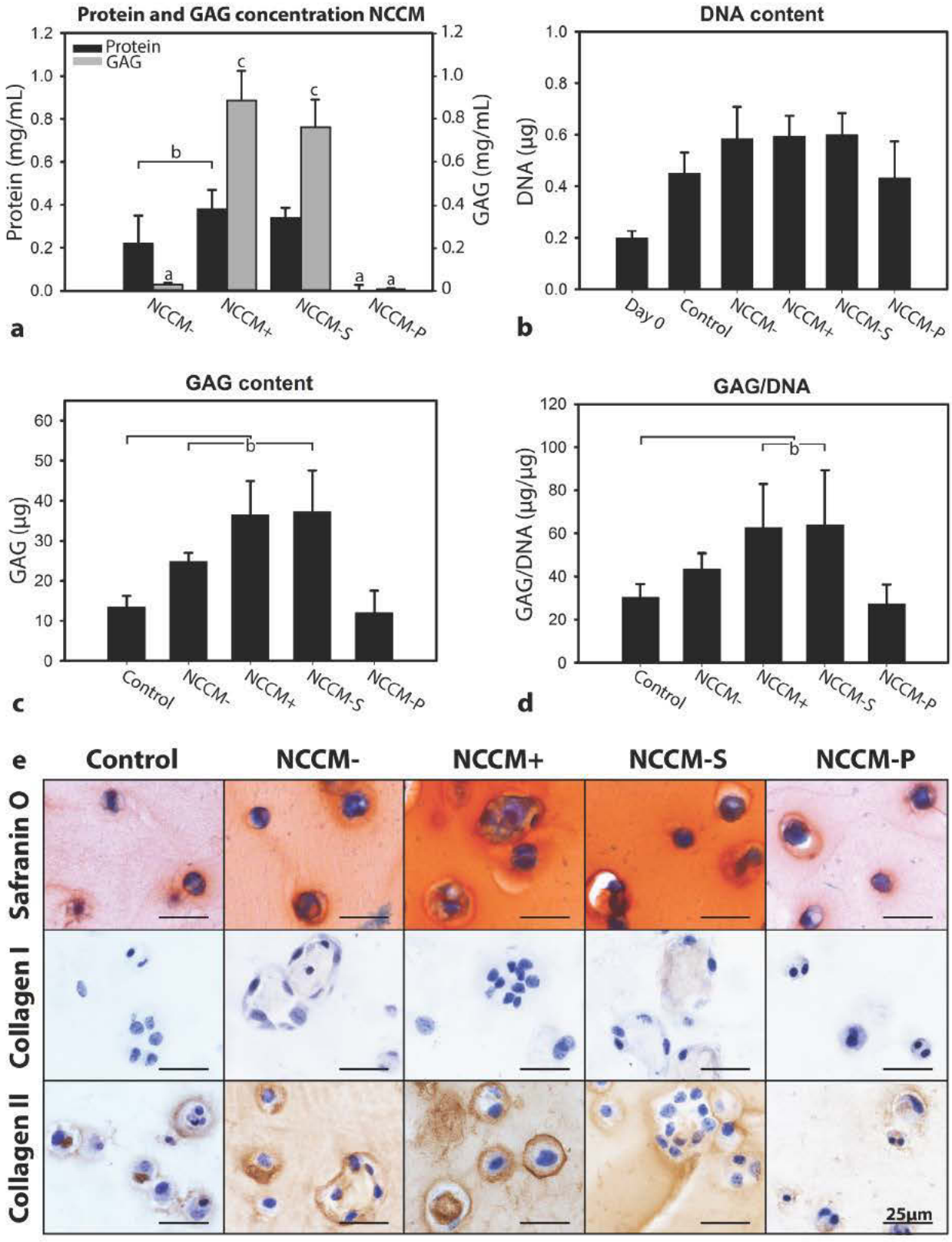

Fig. 2. Soluble factors derived from porcine NC-conditioned medium (NCCM) exert anabolic effects on bovine chondrocyte-like cells (CLCs) derived from caudal intervertebral discs (IVDs). Cell proliferation and matrix production of bovine CLCs cultured in alginate beads in basal culture medium (control), NCCM from dedifferentiated NCs (NCCM−), NCCM from healthy NCs (NCCM+), and the soluble (NCCM-S) and pelletable (NCCM-P) fraction of NCCM+, which were separated by ultracentrifugation. (**a**) Protein (black) and glycosaminoglycan (GAG, grey) concentration (mean ± SD) of porcine NCCM (fractions). (**b-d**) DNA, GAG and GAG/DNA content (mean ± SD) of bovine CLC alginate beads at day 28. (**e**) Safranin O/Fast Green staining and collagen type I and II immunohistochemistry of bovine CLC alginate beads at day 28. a, significant difference between this condition and all other conditions ($p < 0.05$); b, significant difference between these conditions ($p < 0.05$); c, significant difference between this condition and all other conditions except for the other condition indicated with 'c' ($p < 0.05$); $n = 4$.

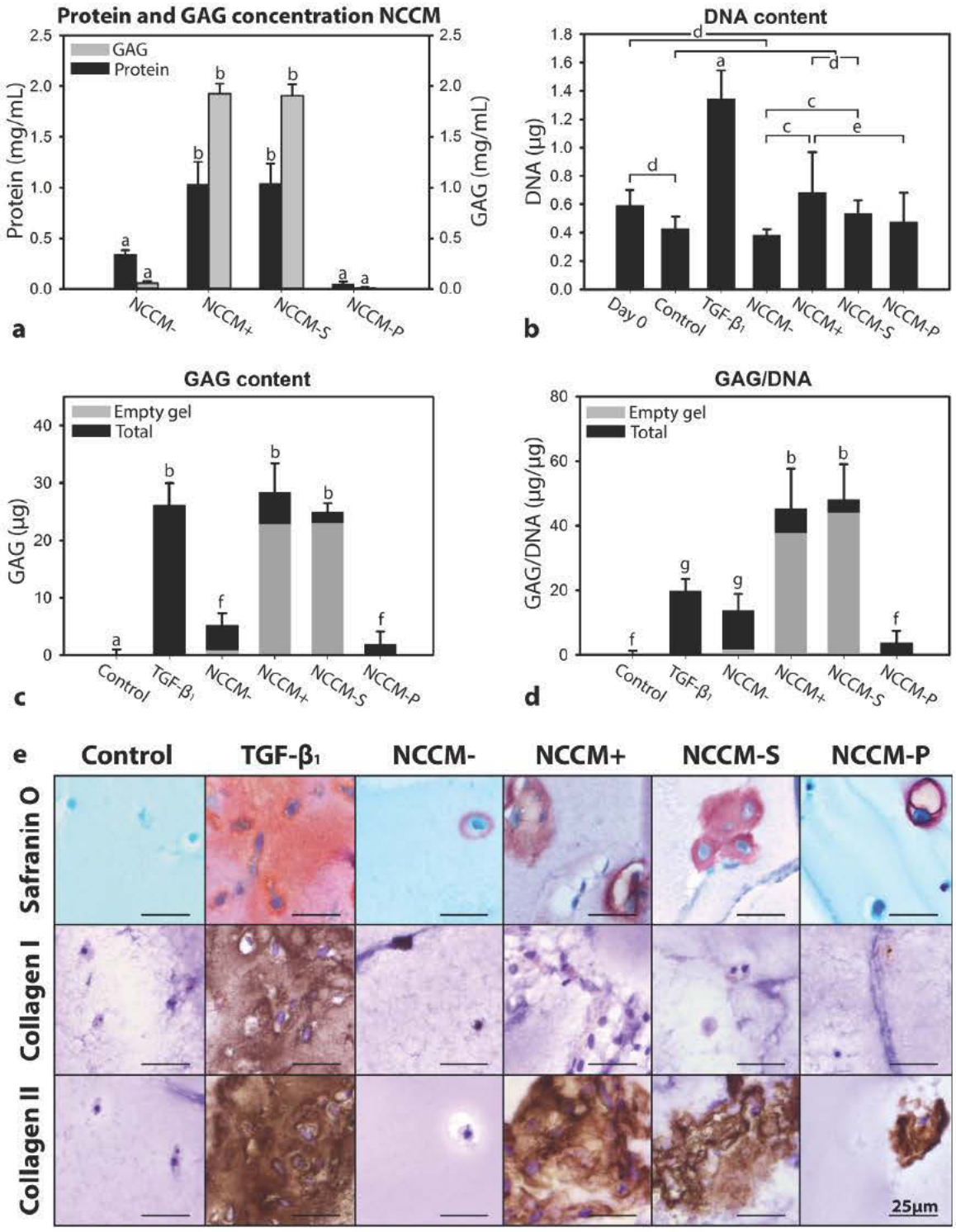

Fig. 3. Both soluble and pelletable factors derived from canine NC-conditioned medium (NCCM) exert anabolic effects on canine chondrocyte-like cells (CLCs) derived from degenerated intervertebral discs (IVDs). Cell proliferation and matrix production of canine CLCs cultured in hydrogels in basal culture medium (control), basal culture medium supplemented with 10 ng/mL TGF-β_1, **NCCM from dedifferentiated NCs (NCCM−), NCCM from healthy NCs (NCCM+), and the soluble (NCCM-S) and pelletable (NCCM-P) fraction of** NCCM+, which were separated by ultracentrifugation. (**a**) Protein (black) and glycosaminoglycan (GAG, grey) concentration (mean ± SD) of canine NCCM (fractions). (**b-d**) DNA, GAG and GAG/DNA content (mean ± SD) of canine CLC hydrogels at day 28. The grey colour in the black bars indicates the level of GAGs present in cell-free NCCM-treated hydrogels for these conditions. (**e**) Safranin O/Fast Green staining and collagen type I and II immunohistochemistry of canine CLC hydrogels at day 28. Significant differences are indicated for non-corrected data (not corrected for empty gels). a, significant difference between this condition and all other conditions ($p < 0.001$); b, significant difference between this condition and all other conditions except for the other condition indicated with 'b' ($p < 0.001$); c, d and e, significant difference between these conditions with $p < 0.001$, $p < 0.01$ and $p < 0.05$, respectively; f and g, significant difference between this condition and all other conditions with $p < 0.01$ and $p < 0.05$, respectively; $n = 8$ for DNA and GAG content and $n = 4$-8 for histology.

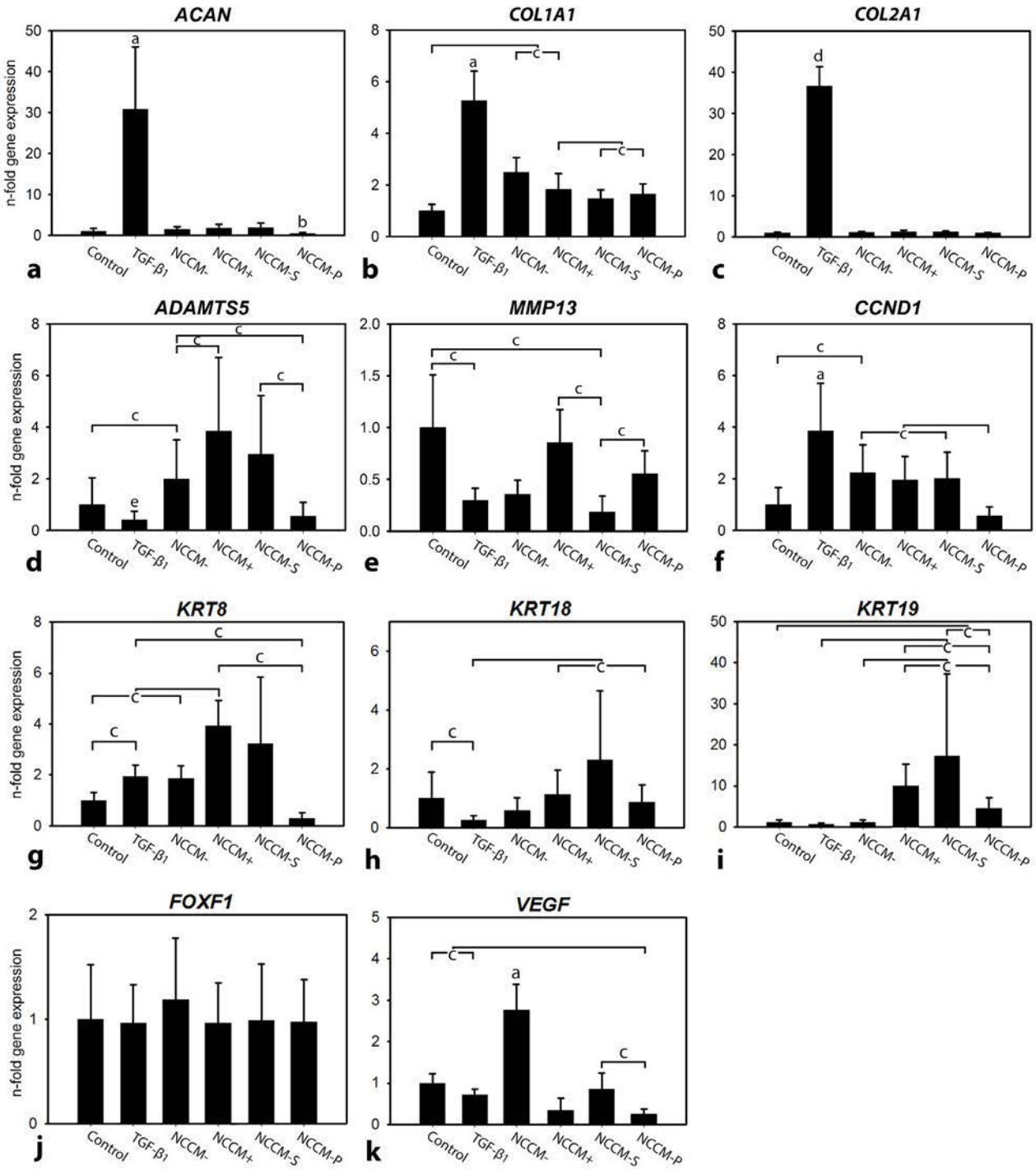

Fig. 4. Only the soluble factors present in canine NC-conditioned medium (NCCM) stimulate expression of genes related to cell proliferation of canine chondrocyte-like cell (CLC), but none of the NCCM (fractions) effects expression of genes related to matrix production. Target gene expression levels of canine CLCs cultured in hydrogels in basal culture medium (control), basal culture medium supplemented with 10 ng/mL TGF-β_1, NCCM from dedifferentiated NCs (NCCM−), NCCM from healthy NCs (NCCM+), and the soluble (NCCM-S) and pelletable (NCCM-P) fraction of NCCM+, which were separated by ultracentrifugation. (**a-k**) Relative *ACAN*, *COL1A1, COL2A1, ADAMTS5, MMP13, CCND1, KRT8, KRT18, KRT19, FOXF1,* and *VEGF* gene expression (mean ± SD) of the hydrogels at day 4. The control hydrogels were set at 1. a, significant difference between this condition and all other conditions ($p < 0.05$); b, significant difference between this condition and all other conditions except control ($p < 0.05$); c, significant difference between these conditions ($p < 0.05$); d, significant difference between this condition and all other conditions ($p < 0.01$); e, significant difference between this condition and all other conditions except NCCM-P ($p < 0.05$); $n = 8$.

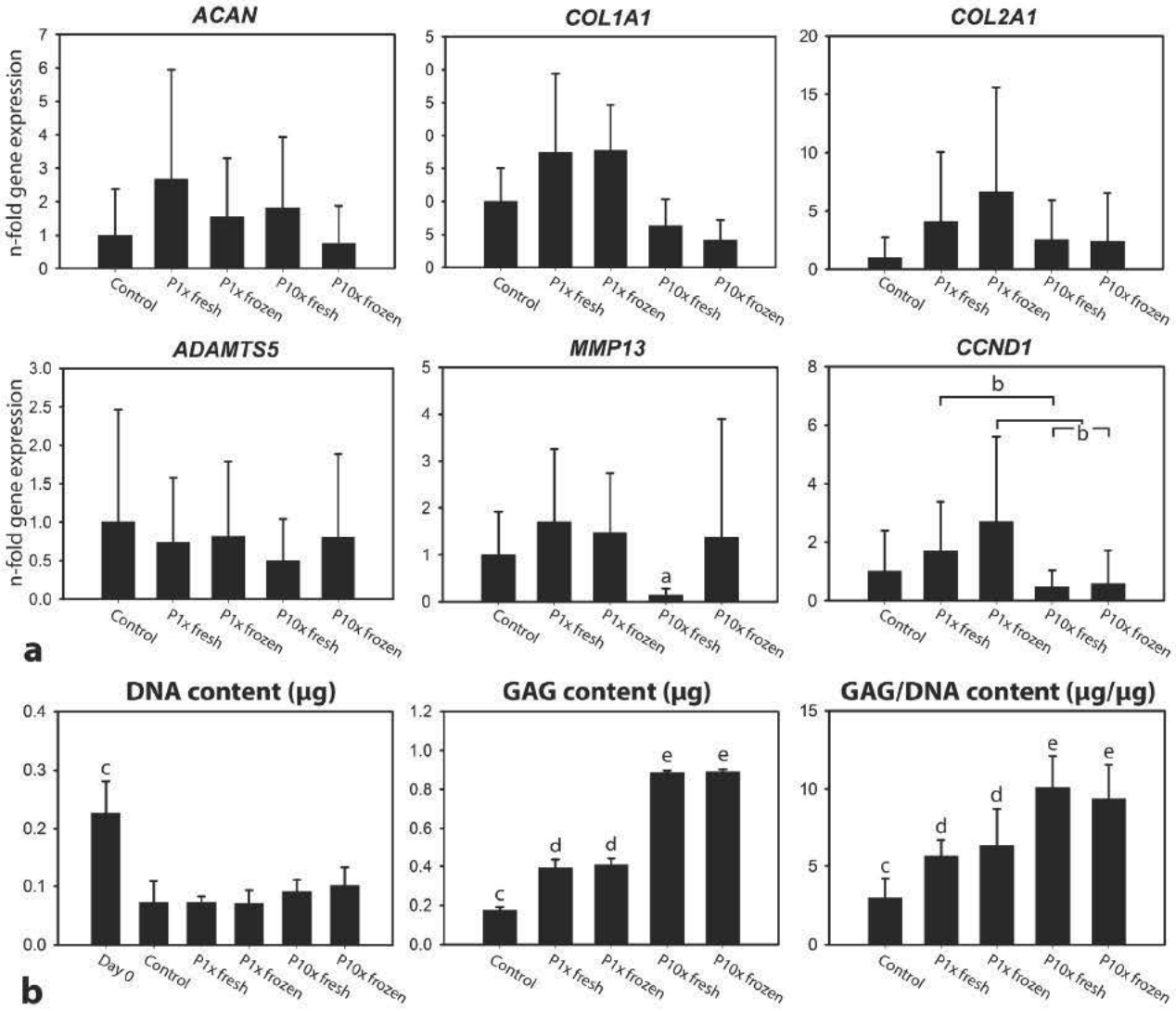

Fig. 5. Frozen canine pelletable NCCM factors exert comparable anabolic effects as freshly applied (non-frozen) pelletable NCCM factors, while a ten times higher concentration of pelletable factors induces a more pronounced effect on canine chondrocyte-like cell (CLC) matrix production. Target gene expression levels and DNA and glycosaminoglycan (GAG) content of canine CLCs cultured in micro-aggregates in basal culture medium (control), or 1× concentrated freshly generated, non-frozen NCCM-P (P1× fresh), 1× concentrated NCCM-P frozen at −70 °C (P1× frozen), 10× concentrated freshly generated, non-frozen NCCM-P (P10× fresh) and 10× concentrated frozen NCCM-P (P10× frozen). (**a**) Relative *ACAN*, *COL1A1, COL2A1, ADAMTS5, MMP13* and *CCND1* gene expression (mean ± SD) of the micro-aggregates at day 4. The control micro-aggregates were set at 1. (**b**) DNA, GAG and GAG/DNA content (mean ± SD) of the canine CLC micro-aggregates at day 7. a, significant difference between this condition and all other conditions ($p < 0.05$); b, significant difference between these conditions ($p < 0.05$); c, significant difference between this condition and all other conditions ($p < 0.01$); d, significant difference between this condition and all other conditions except for the other condition indicated with 'd' ($p < 0.01$); e, significant difference between this condition and all other conditions except for the other condition indicated with 'e' ($p < 0.01$); $n = 8$.

Table 11. Proteins associated with miRNAs in porcine and human NCCM.

	ID	q-value FDR B&H	Hit Count in Query List	Hit Count in Genome	Hit in Query List
Porcine and human	hsa-miR-29b	2.48E-02	7	850	COL3A1, COL5A1, COL5A2, DPYSL2, COL11A1, COL15A1, VCL
Porcine and human	hsa-miR-29a	2.48E-02	7	850	COL3A1, COL5A1, COL5A2, DPYSL2, COL11A1, COL15A1, VCL
Porcine and human	hsa-miR-29c	2.48E-02	7	850	COL3A1, COL5A1, COL5A2, DPYSL2, COL11A1, COL15A1, VCL
Human only	hsa-miR-29c	2.24E-02	4	31	FBN1, FGA, COL1A1, COL1A2

GAG concentration of canine NCCM+ and NCCM-S was significantly higher than that of NCCM− and NCCM-P, whereas the protein and GAG concentration of NCCM-P was significantly lower than that of NCCM− ($p < 0.001$, Fig. 3**a**).

After 4 d of culture, gene expression profiling was performed on the canine CLC-containing hydrogels and after 28 d of culture, the hydrogels were analysed for DNA and GAG content and histology. The DNA content and *CCND1* (a marker for cell proliferation) expression of the TGF-β_1-treated hydrogels was significantly increased compared with all other conditions ($p < 0.05$, Figs. 3**b** and 4**f**). Furthermore, NCCM+ and NCCM-S-treated hydrogels showed a significantly increased DNA content compared with controls, and NCCM+ treatment showed a significantly increased DNA content compared with NCCM-P and NCCM− treatment ($p < 0.05$, Fig. 3**b**). *CCND1* expression was significantly lower in NCCM-P-treated CLCs than in NCCM−/NCCM+/NCCM-S-treated CLCs ($p < 0.05$, Fig. 4**f**).

Using the DMMB assay, empty (no cell-containing) hydrogels were found to incorporate a large amount of NCCM-derived GAGs, indicated by the grey bars in Fig. 3**c**. The GAG content of the control hydrogels was significantly lower than that of all other conditions ($p < 0.001$, Fig. 3**c**). TGF-β_1, NCCM+ and NCCM-S treatment induced the highest total GAG content of the CLC-containing hydrogels: significantly higher than after NCCM− and NCCM-P treatment ($p < 0.001$, Fig. 3**c**). The GAG content of the NCCM-P-treated hydrogels was significantly lower than that of the hydrogels treated with NCCM− ($p < 0.01$, Fig.3**c**). The total GAG/DNA content of NCCM+ and NCCM-S-treated hydrogels was the highest, followed by hydrogels treated with TGF-β_1, NCCM−, NCCM-P and basal culture medium, respectively ($p < 0.05$, Fig. 3**d**). Safranin O/Fast Green staining indicated that most GAGs were deposited in the TGF-β_1-treated hydrogels, followed by NCCM+ and NCCM-S-treated hydrogels (Fig. 3**e**). Collagen type I deposition was only induced by TGF-β_1 treatment, not by NCCM fractions (Fig. 3**e**). Collagen type II was mostly deposited in NCCM+, NCCM-S, and TGF-β_1-treated hydrogels, but also some collagen type II was present in NCCM-P-treated hydrogels (Fig. 3**e**). Affirmatively, at the gene expression level, TGF-β_1 treatment significantly induced *ACAN*, *COL1A1* and *COL2A1* mRNA compared with all other conditions ($p < 0.05$, Fig. 4**a-c**). In contrast, NCCM (fractions) did not influence *COL2A1* expression compared with controls (Fig. 4**a-c**). NCCM-P inhibited *ACAN* expression and NCCM− and NCCM+ induced *COL1A1* expression compared with controls ($p < 0.05$, Fig. 4**a-c**). *COL10A1* expression was not detected in any condition (data not shown).

Furthermore, TGF-β_1 treatment significantly reduced *ADAMTS5* expression compared with all other conditions, whereas NCCM− significantly induced *ADAMTS5* expression compared with controls and NCCM-P ($p < 0.05$, Fig. 4**d**). NCCM+ induced even more *ADAMTS5* expression than NCCM− and NCCM-S increased *ADAMTS5* expression compared with NCCM-P ($p < 0.05$, Fig. 4**d**). *MMP13* expression was significantly decreased by TGF-β_1 treatment compared with controls, whereas NCCM-S reduced *MMP13* expression compared with controls, NCCM+ and NCCM-P ($p < 0.05$, Fig. 4**e**). Expression of the notochordal marker *T* was not detected regardless of the culture condition (data not shown), whereas expression of notochordal marker *KRT8* was significantly higher in micro-aggregates treated with NCCM+ than in micro-aggregates treated with NCCM-P, NCCM−, TGF-β_1 and the negative controls ($p < 0.05$, Fig. 4**g**). Expression of NP marker *KRT18* was significantly increased in micro-aggregates treated with basal culture medium, NCCM+, NCCM-S and NCCM-P compared with TGF-β_1-treated micro-aggregates ($p < 0.05$, Fig. 4**h**). *KRT19* expression was significantly increased by NCCM-P and NCCM-S treatment compared with controls ($p < 0.05$, Fig. 4**i**). Additionally, NCCM+, NCCM-S and NCCM-P treatment significantly increased the expression of this NP marker compared with NCCM− and TGF-β_1 treatment ($p < 0.05$, Fig.4**i**). In contrast, *FOXF1* expression was not influenced by the culture conditions (Fig. 4**j**). Expression of the angiogenic marker *VEGF* was significantly higher in micro-aggregates treated with NCCM− than in all other conditions ($p < 0.05$, Fig. 4**j**). Furthermore, *VEGF* expression was significantly decreased by NCCM-P treatment compared with control, TGF-β_1 and NCCM-S treatment ($p < 0.05$). Apoptosis-related genes (*BAX, BCL2, CASP3*) were not differentially expressed between the conditions (data not shown).

Fresh *versus* frozen pelletable factors present in canine NCCM

Gene expression profiling of CD canine CLC micro-aggregates cultured in basal culture medium (control), 1× concentrated fresh (non-frozen) and frozen NCCM-P and 10× concentrated fresh (non-frozen) and frozen NCCM-P was performed at day 4. Due to donor variability, high standard deviations were obtained (Fig. 5**a**). At day 7, the DNA content of all micro-aggregates was significantly decreased compared with day 0 ($p < 0.01$, Fig 5**b**). The GAG and GAG/DNA content of the controls was significantly lower than that of the micro-aggregates treated with 1× and 10× concentrated NCCM-P ($p < 0.01$, Fig 5**b**). Moreover, the GAG and GAG/DNA content of the micro-aggregates treated with 10× concentrated NCCM-P was significantly higher than that of the micro-aggregates treated with 1× concentrated NCCM-P ($p < 0.01$, Fig 5**b**), indicating a concentration-dependent effect, which could be repeated with frozen NCCM-P. This indicates that freezing the pelletable factors for a short period (1 h – 4 d) at −70 °C in EV-depleted PBS/0.2 % BSA did not affect their biological effect.

Discussion

NCCM exerts cross-species anabolic effects on CLCs

Porcine, canine and human NC-secreted factors have already shown potential for IVD regeneration (Abbott *et al.*, 2012; Bach *et al.*, 2015; de Vries *et al.*, 2016; Gantenbein *et al.*, 2014; Korecki *et al.*, 2010; Purmessur *et al.*, 2011). With a clinical directive in mind, the aim of this study was to delineate underlying bioactive NC-secreted substances

(with the focus on proteins and EVs) resulting in IVD regeneration. The present study shows that porcine and canine NCCM+ have the potential to exert a regenerative effect on bovine and canine CLCs, respectively. Secreted factors from healthy NCs (NCCM+) exerted a more pronounced anabolic effect and induced higher notochord/nucleus pulposus specific marker expression in CLCs than the secreted factors from dedifferentiated NCs (NCCM−), indicating that this was related to preservation of the NC phenotype (Arkesteijn *et al*., 2013).

Proteomic analysis reveals many common proteins in porcine, canine and human NCCM

Since previous findings indicated regenerative effects of porcine, canine and human NCCM on human CLCs (Bach *et al*., 2015), the main focus of the proteomic analysis of this study was on common proteins discovered in NCCM from all three species. A considerable part of the detected proteins consisted of ECM, *e.g.* proteoglycans, collagens and keratins, and organelle-derived proteins. However, specific growth factors, potentially responsible for NCCM's regenerative effect, were not identified, which is in contrast with previous studies in which CTGF was identified in canine (Erwin *et al*., 2006) and porcine (Gantenbein *et al*., 2014) NCCM. This discrepancy may be due to the method of NCCM generation. Whereas the previous studies produced NCCM from isolated NCs, in the current study, NCCM was generated from NC-rich NP tissue. Potential growth factors secreted by NCs may therefore be overshadowed by large quantities of proteins released during NP tissue incubation. In line with previous findings (Purmessur *et al*., 2011), however, clusterin and alpha-2-macroglobulin were detected in all the species' NCCM, and tenascin in human and canine NCCM. These matricellular proteins may have protective effects for NP cells. Furthermore, class 3 semaphorins were identified in canine (SEMA3C, SEMA3E) and porcine (SEMA3C) NCCM. SEMA3C is suggested to play a role in innervation and vascularisation of degenerated human IVDs and has been linked to back pain (Binch *et al*., 2015). The finding of SEMA3C and SEMA3E in canine and porcine NCCM derived from healthy NPs, however, may also support an inhibitory role of semaphorins in nerve and blood vessel growth (Bagnard *et al*., 1998).

The proteins in common to all three species and upstream bioinformatics analysis provide new insights into IVD (patho)physiology, including transcriptional gene regulation. For example, proteins related to transcription factor binding sites AP-1 and PAX4 were identified. AP-1 is a downstream target of the mitogenic activated protein (MAP) kinase signalling pathway and regulates chondrogenic differentiation (Seghatoleslami and Tuan, 2002). In healthy porcine, canine and human NP tissue, GAG synthesis may be regulated in an AP-1/growth factor-dependent manner, given that BMP2 and TGF-β induced the expression of the GAG synthesis enzyme β1,3-glucuronosyl transferase 1 in rat NP cells *via* – amongst others – AP-1 (Hiyama *et al*., 2010). PAX4 has been mainly studied in the pancreas (Mathiyalagan *et al*., 2015; Napolitano *et al*., 2015), whereas its role in bone/cartilaginous tissues is unexplored. PAX1 and PAX9, however, are known to be associated with axial and limb skeleton development (LeClair *et al*., 1999) and vertebral body and cartilage formation (Barnes *et al*., 1996). Furthermore, the current study also demonstrates that proteins related to miR-29a/b/c were present in porcine and human NCCM+. The miR-29 family negatively regulates TGF-β and canonical Wnt signalling (Le *et al*., 2016; Luna *et al*., 2011), exerts anti-fibrotic effects (He *et al*., 2013), and acts across development and progression of osteoarthritis (Le *et al*., 2016). In the IVD, the role of the miR-29 family has not been investigated yet, but based on knowledge from other tissues it could also be involved in ECM production.

Taken together, many common proteins were identified in porcine, canine and human NCCM. Mainly ECM and organelle-derived proteins, but no specific growth factors were detected. Furthermore, in porcine and human NCCM, platelet- and complement system-related proteins were identified. Possibly these proteins were identified as a result of blood contamination explained by the technically challenging harvesting of NP tissue, rather than being a biologically relevant finding. Hence, it may be beneficial for future studies to focus on comparative proteomic analysis of porcine, canine and human NCCM generated from isolated NCs, without interfering ECM proteins.

Pelletable NCCM factors exert a moderate anabolic effect on canine CLCs

Proteomic analysis revealed that NCCM+ contained a considerable amount of membrane-bound vesicle proteins. In functional studies, the effect of NCCM-P (containing EVs and protein aggregates) was determined on CLCs. In bovine CLCs, the effect of porcine NCCM-P factors was negligible. In contrast, canine NCCM-P factors increased, in a concentration-dependent manner, the canine CLC GAG, GAG/DNA and collagen type II content compared with controls (although less pronounced than for the soluble factors). Also, canine NCCM-P decreased *VEGF* and increased *KRT19* expression compared with controls, indicating that it inhibited angiogenesis (Cornejo *et al*., 2015) and induced a healthy NP-like phenotype (Minogue *et al*., 2010). The bovine CLCs were obtained from relatively healthy/early degenerated IVDs and the canine CLCs from degenerated IVDs, which may explain the difference in response, besides NCCM/CLC species differences.

In the present study, NCCM-P needed to be frozen, since canine NCCM donors were available at unpredictable moments. The effect of freezing EVs is controversial: previous studies demonstrated that EVs were relatively insensitive to freeze/thaw cycles (Lorincz *et al*., 2014; Witwer *et al*., 2013), whereas others showed the opposite (Dey-Hazra *et al*., 2010). The current study showed that at least 4 d of freezing at −70 °C did not influence the biological activity of canine NC-derived pelletable factors compared with non-frozen pelletable factors (kept at 4 °C) from the same donor on canine CLC micro-aggregates. Besides long term freezing, also relatively hampered access to the pelletable factors could have accounted for the less

pronounced effect of NCCM-P on the canine hydrogels and bovine alginate beads compared with the canine micro-aggregates.

Taken together, the present study demonstrates that the NCCM-P factors (protein aggregates and EVs) exerted a moderate concentration-dependent anabolic effect, but only on canine CLCs. While we cannot exclude that the absence of a biologic effect of EVs present in the NCCM-P may be related to the 100,000×*g* ultracentrifugation (Nordin *et al.*, 2015), future studies should focus on the effect of different isolation protocols and different populations of purified NC-derived EVs, without interference of protein aggregates present in NCCM-P.

Soluble porcine and canine NCCM factors exert anabolic effects on bovine and canine CLCs

It appeared that most proteins remained in the soluble fraction of canine and porcine NCCM after ultracentrifugation. The effect of porcine NCCM-S on bovine CLCs was similar to that of NCCM+, suggesting that porcine NCCM exerted its anabolic effect mainly through protein-based mechanisms. Also in the canine species, and the GAG content of NCCM-S-treated hydrogels was rather similar to that of hydrogels treated with NCCM+. However, the hydrogel appeared to have the propensity to bind the GAGs present in NCCM. Correcting for this property indicates that NCCM− may be even more active than NCCM+ or NCCM-S. However, this was not evident from the histological analysis. In our view, the amount of GAGs produced by the CLCs themselves cannot simply be calculated by correcting for the GAG content of empty hydrogels cultured in NCCM, because the incorporated ECM proteins likely changed the micro-environment and consequently affected GAG synthesis (Gilchrist *et al.*, 2011; Inoue *et al.*, 2005).

Generally, notochord/nucleus pulposus specific marker expression was higher after NCCM+ and NCCM-S than after NCCM-P treatment, indicating that NCCM+ and NCCM-S were better able to induce a healthy NP phenotype. Furthermore, *ACAN* and *COL2A1* expression did not differ between NCCM-treated CLCs and controls, while *ADAMTS5* and *MMP13* gene expression levels were generally higher in NCCM+ and/or NCCM-S-treated CLCs compared with other conditions. The latter is most probably related to ECM remodelling rather than catabolism, given that histological analysis points towards a stronger anabolic effect of NCCM+ and NCCM-S than NCCM-P and NCCM−. In NCCM+ and NCCM-S, more pericellular GAGs were observed, suggesting that the CLCs synthesised these GAGs themselves. Also collagen type II deposition was highest after NCCM+ and NCCM-S treatment, again indicating that both porcine and canine NCCM exerted their anabolic effects mainly through proteins. Since no blocking experiment was performed, however, it is difficult to discern if one or combination of factors are responsible for the effects of NCCM.

Conclusions

The present study demonstrates an anabolic cross-species effect of porcine and canine NCCM+ on bovine and canine CLCs, respectively. Especially on bovine CLCs, a pronounced effect of the soluble NCCM fraction (NCCM-S; peptides, proteins) was found, without an appreciable effect of the pelletable NCCM fraction (NCCM-P; protein aggregates, EVs). However, NCCM-P exerted a moderate anabolic effect on canine CLCs, although the culture system used precludes firm conclusions. Thus, although porcine and canine NCCM exerted their anabolic effects mainly through soluble factors, also the pelletable NCCM factors showed moderate regenerative potential. Although the regenerative potential of NCCM-P should not be overlooked, future studies should focus on unravelling the protein-based regenerative mechanism from NCCM produced from isolated NCs, *e.g.* by NCCM fractionation and pathway blocking studies.

Acknowledgements

This work was funded by AOSpine International (SRN2011_11) and the Dutch Arthritis Foundation (LLP22). The authors would like to thank Willem de Jong for help with the execution of experiments and Anita Krouwels for supplying human IVDs. We wish to confirm that there are no known conflicts of interest associated with this publication and there has been no significant financial support for this work that could have influenced its outcome.

References

Abbott RD, Purmessur D, Monsey RD, Iatridis JC (2012) Regenerative potential of TGFbeta3 + Dex and notochordal cell conditioned media on degenerated human intervertebral disc cells. J Orthop Res **30**: 482-488.

Anderson HC, Mulhall D, Garimella R (2010) Role of extracellular membrane vesicles in the pathogenesis of various diseases, including cancer, renal diseases, atherosclerosis, and arthritis. Lab Invest **90**: 1549-1557.

Arkesteijn IT, Potier E, Ito K (2013) Maintaining notochordal phenotype. Global Spine Congress 2013, Hong Kong.

Arkesteijn IT, Smolders LA, Spillekom S, Riemers FM, Potier E, Meij BP, Ito K, Tryfonidou MA (2015) Effect of coculturing canine notochordal, nucleus pulposus and mesenchymal stromal cells for intervertebral disc regeneration. Arthritis Res Ther **17**: 60.

Bach FC, Willems N, Penning LC, Ito K, Meij BP, Tryfonidou MA (2014) Potential regenerative treatment strategies for intervertebral disc degeneration in dogs. BMC Vet Res **10**: 3.

Bach FC, de Vries SA, Krouwels A, Creemers LB, Ito K, Meij BP, Tryfonidou MA (2015) The species-specific regenerative effects of notochordal cell-conditioned medium on chondrocyte-like cells derived from degenerated human intervertebral discs. Eur Cell Mater **30**: 132-146.

Bagnard D, Lohrum M, Uziel D, Puschel AW, Bolz J (1998) Semaphorins act as attractive and repulsive

guidance signals during the development of cortical projections. Development **125**: 5043-5053.

Barnes GL, Hsu CW, Mariani BD, Tuan RS (1996) Chicken Pax-1 gene: structure and expression during embryonic somite development. Differentiation **61**: 13-23.

Benneker LM, Andersson G, Iatridis JC, Sakai D, Hartl R, Ito K, Grad S (2014) Cell therapy for intervertebral disc repair: advancing cell therapy from bench to clinics. Eur Cell Mater **27**: 5-11.

Benz K, Stippich C, Osswald C, Gaissmaier C, Lembert N, Badke A, Steck E, Aicher WK, Mollenhauer JA (2012) Rheological and biological properties of a hydrogel support for cells intended for intervertebral disc repair. BMC Musculoskelet Disord **13**: 54.

Binch AL, Cole AA, Breakwell LM, Michael AL, Chiverton N, Creemers LB, Cross AK, Le Maitre CL (2015) Class 3 semaphorins expression and association with innervation and angiogenesis within the degenerate human intervertebral disc. Oncotarget **6**: 18338-18354.

Bolstad BM (2016) Package 'preprocessCore': a collection of pre-processing functions Version 1.33.0.

Carlson M (2016) GO.db: A set of annotation maps describing the entire Gene Ontology. R package version 3.2.2.

Chen H (2015) Package 'VennDiagram': Generate high-resolution Venn and Euler plots.

Chen J, Bardes EE, Aronow BJ, Jegga AG (2009) ToppGene Suite for gene list enrichment analysis and candidate gene prioritization. Nucleic Acids Res **37**: W305-311.

Cheung KM, Karppinen J, Chan D, Ho DW, Song YQ, Sham P, Cheah KS, Leong JC, Luk KD (2009) Prevalence and pattern of lumbar magnetic resonance imaging changes in a population study of one thousand forty-three individuals. Spine **34**: 934-940.

Cornejo MC, Cho SK, Giannarelli C, Iatridis JC, Purmessur D (2015) Soluble factors from the notochordal-rich intervertebral disc inhibit endothelial cell invasion and vessel formation in the presence and absence of pro-inflammatory cytokines. Osteoarthritis Cartilage **23**: 487-496.

de Graaf EL, Giansanti P, Altelaar AF, Heck AJ (2014) Single-step enrichment by $Ti4^{+}$-IMAC and label-free quantitation enables in-depth monitoring of phosphorylation dynamics with high reproducibility and temporal resolution. Mol Cell Proteomics **13**: 2426-2434.

de Vries SA, Potier E, van Doeselaar M, Meij BP, Tryfonidou MA, Ito K (2015) Conditioned medium derived from notochordal cell-rich nucleus pulposus tissue stimulates matrix production by canine nucleus pulposus cells and bone marrow-derived stromal cells. Tissue Eng Part A **21**: 1077-1084.

de Vries SA, van Doeselaar M, Meij BP, Tryfonidou MA, Ito K (2016) The stimulatory effect of notochordal cell-conditioned medium in a nucleus pulposus explant culture. Tissue Eng Part A **22**: 103-110.

Dey-Hazra E, Hertel B, Kirsch T, Woywodt A, Lovric S, Haller H, Haubitz M, Erdbruegger U (2010) Detection of circulating microparticles by flow cytometry: influence of centrifugation, filtration of buffer, and freezing. Vasc Health Risk Manag **6**: 1125-1133.

Durinck S, Spellman PT, Birney E, Huber W (2009) Mapping identifiers for the integration of genomic datasets with the R/Bioconductor package biomaRt. Nat Protoc **4**: 1184-1191.

Erwin WM, Ashman K, O'Donnel P, Inman RD (2006) Nucleus pulposus notochord cells secrete connective tissue growth factor and up-regulate proteoglycan expression by intervertebral disc chondrocytes. Arthritis Rheum **54**: 3859-3867.

Farndale RW, Sayers CA, Barrett AJ (1982) A direct spectrophotometric microassay for sulfated glycosaminoglycans in cartilage cultures. Connect Tissue Res **9**: 247-248.

Gantenbein B, Calandriello E, Wuertz-Kozak K, Benneker LM, Keel MJ, Chan SC (2014) Activation of intervertebral disc cells by co-culture with notochordal cells, conditioned medium and hypoxia. BMC Musculoskelet Disord **15**: 422.

Gilchrist CL, Darling EM, Chen J, Setton LA (2011) Extracellular matrix ligand and stiffness modulate immature nucleus pulposus cell-cell interactions. PLoS One **6**: e27170.

Guo JF, Jourdian GW, MacCallum DK (1989) Culture and growth characteristics of chondrocytes encapsulated in alginate beads. Connect Tissue Res **19**: 277-297.

He Y, Huang C, Lin X, Li J (2013) MicroRNA-29 family, a crucial therapeutic target for fibrosis diseases. Biochimie **95**: 1355-1359.

Hiyama A, Gogate SS, Gajghate S, Mochida J, Shapiro IM, Risbud MV (2010) BMP-2 and TGF-beta stimulate expression of beta1,3-glucuronosyl transferase 1 (GlcAT-1) in nucleus pulposus cells through AP1, TonEBP, and Sp1: role of MAPKs. J Bone Miner Res **25**: 1179-1190.

Inoue T, Nakamura T, Ikeda T, Takagi K (2005) Effect of extracellular matrix protein on the rate of proteoglycan synthesis in rabbit intervertebral disc cells. J Spinal Disord Tech **18**: 52-57.

Korecki CL, Taboas JM, Tuan RS, Iatridis JC (2010) Notochordal cell conditioned medium stimulates mesenchymal stem cell differentiation toward a young nucleus pulposus phenotype. Stem Cell Res Ther **1**: 18.

Le LT, Swingler TE, Crowe N, Vincent TL, Barter MJ, Donell ST, Delany AM, Dalmay T, Young DA, Clark IM (2016) The microRNA-29 family in cartilage homeostasis and osteoarthritis. J Mol Med **94**: 583-596.

LeClair EE, Bonfiglio L, Tuan RS (1999) Expression of the paired-box genes Pax-1 and Pax-9 in limb skeleton development. Dev Dyn **214**: 101-115.

Lorincz AM, Timar CI, Marosvari KA, Veres DS, Otrokocsi L, Kittel A, Ligeti E (2014) Effect of storage on physical and functional properties of extracellular vesicles derived from neutrophilic granulocytes. J Extracell Vesicles **3**: 25465.

Luna C, Li G, Qiu J, Epstein DL, Gonzalez P (2011) Cross-talk between miR-29 and transforming growth factor-betas in trabecular meshwork cells. Invest Ophthalmol Vis Sci **52**: 3567-3572.

Luoma K, Riihimaki H, Luukkonen R, Raininko R, Viikari-Juntura E, Lamminen A (2000) Low back pain in relation to lumbar disc degeneration. Spine **25**: 487-492.

Mahmoudabady M, Niazmand S, Shafei MN, McEntee K (2013) Investigation of apoptosis in a canine model of chronic heart failure induced by tachycardia. Acta Physiol Hung **100**: 435-444.

Malda J, Boere J, van de Lest CH, van Weeren PR, Wauben MH (2016) Extracellular vesicles – new tool for joint repair and regeneration. Nat Rev Rheumatol **12**: 243-249.

Marino F, Cristobal A, Binai NA, Bache N, Heck AJ, Mohammed S (2014) Characterization and usage of the EASY-spray technology as part of an online 2D SCX-RP ultra-high pressure system. Analyst **139**: 6520-6528.

Mathiyalagan P, Keating ST, Al-Hasani K, El-Osta A (2015) Epigenetic-mediated reprogramming of pancreatic endocrine cells. Antioxid Redox Signal **22**: 1483-1495.

Minogue BM, Richardson SM, Zeef LA, Freemont AJ, Hoyland JA (2010) Characterization of the human nucleus pulposus cell phenotype and evaluation of novel marker gene expression to define adult stem cell differentiation. Arthritis Rheum **62**: 3695-3705.

Muir P, Danova NA, Argyle DJ, Manley PA, Hao Z (2005) Collagenolytic protease expression in cranial cruciate ligament and stifle synovial fluid in dogs with cranial cruciate ligament rupture. Vet Surg **34**: 482-490.

Napolitano T, Avolio F, Courtney M, Vieira A, Druelle N, Ben-Othman N, Hadzic B, Navarro S, Collombat P (2015) Pax4 acts as a key player in pancreas development and plasticity. Semin Cell Dev Biol **44**: 107-114.

Nordin JZ, Lee Y, Vader P, Mager I, Johansson HJ, Heusermann W, Wiklander OP, Hallbrink M, Seow Y, Bultema JJ, Gilthorpe J, Davies T, Fairchild PJ, Gabrielsson S, Meisner-Kober NC, Lehtio J, Smith CI, Wood MJ, El Andaloussi S (2015) Ultrafiltration with size-exclusion liquid chromatography for high yield isolation of extracellular vesicles preserving intact biophysical and functional properties. Nanomedicine **11**: 879-883.

Potier E, de Vries S, van Doeselaar M, Ito K (2014) Potential application of notochordal cells for intervertebral disc regeneration: an *in vitro* assessment. Eur Cell Mater **28**: 68-80.

Purmessur D, Schek RM, Abbott RD, Ballif BA, Godburn KE, Iatridis JC (2011) Notochordal conditioned media from tissue increases proteoglycan accumulation and promotes a healthy nucleus pulposus phenotype in human mesenchymal stem cells. Arthritis Res Ther **13**: R81.

Purmessur D, Cornejo MC, Cho SK, Hecht AC, Iatridis JC (2013) Notochordal cell-derived therapeutic strategies for discogenic back pain. Global Spine J **3**: 201-218.

Sakai D, Andersson GB (2015) Stem cell therapy for intervertebral disc regeneration: obstacles and solutions. Nat Rev Rheumatol **11**: 243-256.

Sakai D, Grad S (2015) Advancing the cellular and molecular therapy for intervertebral disc disease. Adv Drug Deliv Rev **84**: 159-171.

Scholz B, Kinzelmann C, Benz K, Mollenhauer J, Wurst H, Schlosshauer B (2010) Suppression of adverse angiogenesis in an albumin-based hydrogel for articular cartilage and intervertebral disc regeneration. Eur Cell Mater **20**: 24-36.

Seghatoleslami MR, Tuan RS (2002) Cell density dependent regulation of AP-1 activity is important for chondrogenic differentiation of C3H10T1/2 mesenchymal cells. J Cell Biochem **84**: 237-248.

van der Vlist EJ, Nolte-'t Hoen EN, Stoorvogel W, Arkesteijn GJ, Wauben MH (2012) Fluorescent labeling of nano-sized vesicles released by cells and subsequent quantitative and qualitative analysis by high-resolution flow cytometry. Nat Protoc **7**: 1311-1326.

Witwer KW, Buzas EI, Bemis LT, Bora A, Lasser C, Lotvall J, Nolte-'t Hoen EN, Piper MG, Sivaraman S, Skog J, Thery C, Wauben MH, Hochberg F (2013) Standardization of sample collection, isolation and analysis methods in extracellular vesicle research. J Extracell Vesicles **2**: 10.3402/jev.v2i0.20360.

Discussion with Reviewers

Reviewer II: Notochordal cells (NCs) were associated with the occurrence of chordoma, a mostly benign form of spine cancer. Chordomas are thought to arise from remnants of the embryonic notochord. Thus, the lack of NC in adults seems to be highly relevant for a healthy development. The authors assumedly aim for a therapeutic drug isolated from the secretome of the NC, the so-called conditioned medium (NCCM). Cancer cells often influence their neighbouring cells by a specific signalling. What would be the authors' vision to deliver such a signalling molecule to the intervertebral disc and what risks do the authors see for clinical application?

Authors: Since chordomas are thought to arise from the embryonic notochord, the application of notochord-/notochordal cell-derived factors could theoretically induce chordoma formation. However, it is unclear which initiating mechanisms are crucial for chordoma development when notochordal remnants persist. Also, the prevalence of chordoma in humans (and mice) is very low (1 in 1,000,000 people) (Lawson and Harfe, 2015). In line with this, in the clinics we (almost) never see tumours arising from the nucleus pulposus in non-chondrodystrophic dogs, and these dogs do retain their NCs until late in life (Smolders *et al.*, 2013) and can develop several other types of cancer. This altogether suggests that the vast majority of notochord cells or their remnants do not result in disease. Nonetheless, when screening for potential regenerative NC-secreted factors, factors that are known to be associated with cancer formation should be carefully investigated in this respect.

Additional References

Lawson L, Harfe BD (2015) Notochord to nucleus pulposus transition. Curr Osteoporos Rep **13**: 336-341.

Smolders LA, Bergknut N, Grinwis GC, Hagman R, Lagerstedt AS, Hazewinkel HA, Tryfonidou MA, Meij BP (2013) Intervertebral disc degeneration in the dog. Part 2: chondrodystrophic and non-chondrodystrophic breeds. Vet J **195**: 292-299.

Editor's note: The Scientific Editor responsible for this paper was Mauro Alini.